TWO TOPICS IN THE PHYSICS OF THE SOLAR WIND:

1) A Model of Fermi Acceleration at Shock Fronts.

2) Effects of Diffusion on the Composition of the Solar Corona and Solar Wind.

Thesis by

J. R. Jokipii

In Partial Fulfillment of the Requirements
For the Degree of
Doctor of Philosophy

California Institute of Technology
Pasadena, California
1965
(Submitted May 25, 1965)

ACKNOWLEDGEMENTS

I am happy to acknowledge the continued interest and encouragement of my advisor, Professor Leverett Davis, Jr.

I am also indebted to Dr. D. Burnett of the High Altitude Observatory for informative discussions concerning diffusion and also for providing me with results before publication. Dr. George Siscoe patiently served as a sounding board for many ideas contained in this thesis.

Financial support of the National Science Foundation in the form of graduate fellowships is gratefully acknowledged.

ABSTRACT

1. A Model of Fermi Acceleration at Shock Fronts

A model of first order Fermi acceleration at shock fronts is developed. A "fast" hydromagnetic shock is assumed to be propogating toward an isolated magnetic mirror in an otherwise uniform magnetic field which is not parallel to the shock front. The behavior of an ensemble of particles trapped between the mirror and the shock is studied and a differential equation describing the balance of particle injection into the trapping region, loss through the shock or mirror, and energy gain is obtained. A general expression for n(W, t), the number of trapped particles as a function of energy and time is obtained. Useful limiting forms are discussed. Possible sources of particles eligible for acceleration are discussed and an attractive source is shown to be the quasi-thermalized plasma behind the shock, a small fraction of which may leak out in front of the shock and be accelerated. The flux of particles through the shock is found to be small and due mainly to convection with magnetic irregularities behind the shock. The energy spectrum of accelerated particles behind the shock is therefore expected to be nearly the same as in the trapping region.

The general theory is then applied to the acceleration of electrons at the earth's bow shock. This leads to an attractive model for the energetic electron pulses which have been observed beyond the magnetopause. The observations and their interpretation are discussed. If a small fraction of the ~ 1 keV electrons in the quasi-thermalized plasma behind the shock escape to the region in front of the shock, many quantitative features of the observed pulses are explained by a model in which each pulse is due to the acceleration of these electrons by a mirror approaching the bow shock. In particular, the cutoff in >30 keV pulses at a few earth radii beyond the shock is readily explained. The theory predicts, further, that cutoffs for more energetic particles should be at smaller distances from the shock. The observed energy spectra are in excellent agreement with the model. Some critical observations are suggested.

2. Effects of Diffusion on the Composition of the Solar Corona and Solar Wind

A simple model is developed with which it is possible to estimate quantitatively the effects of radial diffusion on the composition of the solar corona and solar wind. As it flows out to form the solar wind, it is assumed that each constituent satisfies the time independent equation of continuity $n_t v_t r^2$ = constant, where n_t and v_t are the number density and velocity of element t at heliocentric radius r. For typical coronal temperatures of 1 - 2 x 10^6 ^oK and solar wind fluxes of 3 x 10^8 protons $cm^{-2}sec^{-1}$ at r = 1 AU, the relative diffusion velocities of ions and protons are a substantial fraction of the local solar wind velocity. This diffusion is found to be mostly due to the coronal pressure gradient, with the effect of the temperature gradient relatively unimportant. The large relative velocities together with the above continuity equation lead to substantial changes in the relative composition of the solar wind. Effects of magnetic fields and turbulent mixing are briefly considered. It is concluded that, in conjunction with the diffusion, they may lead to appreciable fluctuations of the composition as a function of time and heliocentric radius. The conclusions are in agreement with the observed behavior of the He/H ratio observed on Mariner-2.

Table of Contents

A Model of Fermi Acceleration at Shock Fronts

I. Introduction

The first part of this thesis developes a simple theory of charged particle acceleration by hydromagnetic shock fronts. The discussion is a development of some ideas recently suggested by Jokipii and Davis (1964), who proposed Fermi acceleration at the earth's bow shock as a promising explanation of energetic electron pulses observed beyond the magnetopause (Fan, Gloeckler and Simpson, 1964; Anderson, Harris and Paoli, 1964; Frank and Van Allen, 1964; and Montgomery, Singer, Conner and Stogsdill, 1965). The present discussion is split into two parts. First, a general approach to the behavior of particles trapped between a shock and a magnetic mirror is developed. A differential equation, describing the average behavior of an ensemble of trapped particles in energy and time, is derived and a general solution presented. Useful limiting forms of the solution are discussed. Finally, conditions required for the acceleration of particles are discussed and possible sources of eligible particles considered. The second part of the paper is devoted to an application of the theory to the interpretation of energetic electron pulses observed beyond the magnetosphere.

Central to much of contemporary astrophysics is the problem of electromagnetic acceleration of charged particles. Two basic acceleration mechanisms involving large scale magnetic fields have been applied in many models. They are betatron acceleration in an increasing magnetic field as proposed by Swann (1933), and the Fermi mechanism involving interaction with moving magnetic irregularities (Fermi, 1949; 1954). Most attention has been directed toward statistical aspects of the Fermi mechanism and the question of how rapidly particles gain energy over a sequence of many interactions. Shock fronts have been introduced mainly as a mechanism for scattering particles in pitch angle (Parker, 1958). Wentzel (1963) and Parker (1958) have also considered statistical aspects of acceleration between series of converging shocks. Axford and Reid (1963) have suggested that compression of energetic protons between the earth's bow shock and an approaching interplanetary shock front may explain certain polar-cap absorption events, although a detailed model was not worked out. We are interested here in the general problem of first order Fermi acceleration of particles trapped between a single plane shock front and an isolated magnetic irregularity (which may or may not be another shock) moving toward it.

Because much of the following discussion depends on the existence of a shock front in an essentially collisionless plasma, a brief digression on the nature of the assumed shock is in order. Observations point to the existence of irreversible changes in fluid parameters, analogous to fluid dynamical shocks, in collisionless magnetized plasmas such as the solar wind (Ness, Scearce and Seek, 1964; Bridge et al., 1964 and Sonett et al., 1964). Although it is not yet clear to what extent the fluid dynamical analogy is correct for such a shock, fluid dynamical terms will be used below to describe it. None of the results derived, however, depend on a definite model of a shock - all that is required is the observed relatively thin propogating front, behind which there is turbulent magnetic field and quasi-thermalized plasma.

II. Acceleration of Charged Particles

Consider a situation in which a shock propagates into a magnetic field $\underset{\sim}{B}_0$ which is not parallel to the (locally) plane shock front. There then exists a coordinate system in which the shock front is stationary and the plasma flow velocity is either parallel or antiparallel to the average magnetic field on either side of the shock (Bazer and Ericson, 1959). We will work entirely in this coordinate system. $\underset{\sim}{B}_0$, the magnetic field on the side in which the plasma flows toward the shock, is assumed uniform except for a small region of irregular field ($B_M > B_0$) which acts as a magnetic mirror and which is a distance $L(t) = L_0 - \beta_0 c(t - t_0)$ along $\underset{\sim}{B}_0$ from the shock. The mirror may be stationary with respect to the incoming plasma, in which case $\beta_0 c$ is simply the plasma flow velocity; or the mirror may be moving relative to the plasma so that $\beta_0 c$ may differ from the plasma velocity. We further require the shock to be analogous to a "fast" hydromagnetic shock (Bazer and Ericson, 1959), for which the average post-shock magnetic field intensity B_1 is greater than B_0. An energetic particle incident from B_0 onto either B_1 or B_M may be reflected from the region of stronger field and be trapped for a while between the shock and the mirror. Suppose for the present that the mirror conserves the magnetic moment of the particle. The interaction of such a particle with a moving magnetic mirror is discussed in the first appendix. It is found that in the limit that $\beta_0{}^2$ can be neglected compared to unity and the particle velocity $v_p >> c\beta_0$, each reflection from the mirror increases the particle's parallel momentum $P_{\|}$ and changes the particle's total energy W by

$2\beta_0 cP_{\|}$. The reflection from the shock front is more complex, and a general treatment would require detailed knowledge of the shock structure. In the reference system chosen the average electric fields at the shock are curl free and we assume the particle gains, on the average, no energy upon reflection at the shock front. Under the assumption that a particle with pitch angle $\theta_p = \cos^{-1} |P_{\|}/P| = \cos^{-1}\mu$ makes $\mu v_p/2L(t)$ round trips per second, where $v_p = c\sqrt{1 - \frac{m_0^2 c^4}{W^2}}$ is the particle velocity, the particle increases its energy at the rate

$$\frac{dW}{dt} = \beta_0 c \frac{\mu^2}{L(t)} W(1 - \frac{1}{W^2}) \qquad (1)$$

where W has been expressed in units of m_0c^2. In general $L(t)$ will depend upon μ and the structure of the mirror field. Below we will be considering many particles, assuming their average behavior at a given energy W to be given by equation (1) averaged over pitch angle. We therefore refer to an average $L(t)$. As $L(t) = L_0 - \beta_0 c(t - t_0)$ approaches the particle gyroradius r_g, equation (1) begins to break down and the rate of energy gain is no longer simply related to $L(t)$.

In addition, we will neglect collisions with the ambient plasma. In section 3, below, the restrictions this places on the ambient plasma and magnetic field configuration are considered and possible sources of particles eligible for acceleration are discussed.

In Appendix I the conditions under which a moving magnetic mirror reflects particles are discussed. If β_0^2 can be neglected compared to unity, the mirror in general reflects those particles for which, in B_0, $\mu < \mu_c$ where μ_c is given by:

$$\frac{(1 - \mu_c^2)}{\left(\mu_c + \beta_0 \sqrt{1 + \frac{m_0^2 c^4}{P^2}}\right)^2} = \frac{B_0/B_M}{1 - B_0/B_M} \tag{2}$$

and allows all others to be transmitted. Note that as the particle velocity v_p becomes less than or of the order of $c\beta_0$, this is a very stringent condition on μ and few particles are reflected. We are chiefly interested in the other limit, $v_p/c\beta_0 >> 1$, for which equation (2) reduces to $\mu < \sqrt{1 - B_0/B_M}$. If the shock front also conserved the magnetic moment, a particle would gain energy at the rate given by equation (1), but the attendant increase of $\mu = |P_{||}/P|$ would lead to loss of the particle at a relatively low energy. If, however, the shock were thin compared with r_g, the gyroradius, or if the fields at the shock fluctuate rapidly, the particle would be scattered in pitch angle. Since it may be scattered to larger pitch angle (smaller μ), it then is possible to accelerate particles to very high energies. Similarly, if the mirror violated the magnetic moment of the particle, there would be scattering in pitch angle at the mirror. In the latter case, equation (1) may not be correct for each particle. It appears reasonable, however, that the average of equation (1) over a large number of trapped particles may be a reasonable approximation to the average rate of energy gain. The validity of equation (1) for $L(t) \gtrsim r_g$ will be assumed in what follows.

We are therefore led to consider an ensemble of trapped particles. Let $n(W, t)dW$ be the total number of particles with energy in the range W to $W + dW$ which are found in the trapping region at time t, per cm^2 normal to B_0. Then $\rho_t(W, t) = \frac{n(W, t)}{L(t)}$ gives the number density of trapped particles. The average energy gain per particle of energy W is assumed to be given by equation (1) if it is averaged over pitch angle. We neglect the spread in energy caused by the spread in μ over the ensemble. This requires that particles be stirred sufficiently in pitch angle that, after many reflections, it is unlikely that a particle has gained appreciably more or less than the average energy. Suppose that scattering is quite efficient and the particle gains $\delta W = < \delta W > \pm F$ per cycle, where F is of the order of $< \delta W >$ and is assumed to be completely uncorrelated from cycle to cycle. If it is first assumed that F and $< \delta W >$ are constant, a straightforward application of a random walk analysis yields the familiar result that if ΔW is the energy change in N cycles, $< \Delta W^2 > - < \Delta W >^2 \simeq NF^2 \simeq N < \delta W >^2$. Since $< \Delta W > = N < \delta W >$, the r. m. s. fluctuation $\pm \sqrt{N} < \delta W >$ is relatively unimportant for large N. A similar analysis may be carried out if $< \delta W >$ is a slowly varying function of energy. We are therefore apparently justified in neglecting the fluctuations about $< \Delta W >$.

To account for the loss of particles, introduce a loss factor X, defined as the probability per cycle that a particle is scattered into the loss cone of the mirror or otherwise lost from the trapping region.

If the scattering were sufficient to keep the pitch angle distribution nearly isotropic, the loss at the mirror would be X_i. In the limit that the particle velocity $v_p \gg c\beta_0$, it is shown in the first appendix that $X_i \simeq 1 - \sqrt{1 - B_0/B_M}$. Since it is unlikely that particles are preferentially scattered into the loss cone of the mirror, we may conclude that X_i represents an upper bound on X. For X_i assumes that on each cycle the loss cone is uniformly populated; but if scattering or the change in pitch angle due to acceleration are insufficient to "refill" the loss cone on each succeeding cycle, the fraction of particles in the loss cone may be substantially less than in the isotropic case. It is therefore probable that $X \lesssim X_i$.

If particles in the energy range W to W + dW are introduced into the trapping region at a rate S(W, t)dW $cm^{-2}sec^{-1}$, the conservation of particles may be expressed, in terms of the above definitions, as

$$\frac{\partial n}{\partial t} = - \frac{\partial}{\partial W} \left[\frac{aW}{L(t)} \left(1 - \frac{1}{W^2}\right) n \right] - \frac{b}{L(t)} \sqrt{1 - \frac{1}{W^2}} \; n + S(W, t), \quad (3)$$

where for convenience W is again expressed in units of m_0c^2 and we have defined $a = \beta_0 c \langle\mu^2\rangle$, $b = \frac{cX}{2} \langle\mu\rangle$ which will be assumed constants, independent of W and t. The general solution to equation (3) is readily obtained in terms of an integral of the Green's function n_G over the source function, as is discussed in Appendix II. The boundary conditions are chosen to correspond to the physical situation in which there are no trapped particles at $t = t_0$. At this time, either S is turned on, or S is nonzero but the magnetic mirror becomes connected to the shock. Also, we assume no trapped particles of zero kinetic energy. Thus, equation (3) is to be solved for $t > t_0$, $W > 1$ with $n(W, t_0) = n(1, t) = 0$. The general solution is derived in the 2nd appendix and can be expressed formally as

$$n(W, t) = \frac{WL(t)}{(W^2 - 1)^{\left(1 - \frac{1}{2 < \mu^2 >}\right)}} \left[W + \sqrt{W^2 - 1}\right]^{-\frac{b}{a}} \int_1^{\infty} \theta(W - W_1)$$

$$\frac{\left[W_1 + \sqrt{W_1^2 - 1}\right]^{\frac{b}{a}}}{a(W_1^2 - 1)^{\frac{1}{2 < \mu^2 >}}} S(W, t^1)\, \theta \left[\left(\frac{L(t)}{L_0}\right)^{-2 < \mu^2 >} - \frac{W^2 - 1}{W_1^2 - 1}\right] dW_1 \tag{4a}$$

where $$t^1 = \frac{L_0}{\beta_0 c} + \left(\frac{W^2 - 1}{W_1^2 - 1}\right)^{\frac{1}{2 < \mu^2 >}} \left(t - t_0 - \frac{L_0}{\beta_0 c}\right) + t_0 \tag{4b}$$

and the step function $\theta(X) = 1$ if $X > 0$; 0 if $X < 0$. Obviously $n(W, t)$ may be quite complex, but it is in principle obtainable from equation (4) if $S(W, t)$ is known. In spite of the complexity of (4), some very useful results can be obtained if reasonable, heuristic assumptions are made concerning $S(W, t)$.

If, as may usually be expected, $S(W, t)$ has a cutoff energy W_2, above which S is essentially zero, it then follows from equation (4) that there is a corresponding cutoff in $n(W, t)$ at $W_{max}(t)$, where

$$\frac{W_{max}^{2}(t) - 1}{W_{2}^{2} - 1} = \left[\frac{L(t)}{L_0} \right]^{-2 < \mu^2 >} \tag{5}$$

This cutoff energy, which increases as the mirror approaches the shock, is due to the requirement that a particle make many round trips of duration $2L(t)/c\sqrt{1 - \frac{1}{W^2}} < \mu >$ to increase its energy. This result may also be derived by a direct application of equation (1).

It is also quite reasonable that $S(W, t)$ have in addition a lower cutoff at $W_1 > 1$, below which it is also zero. If $S(W, t)$ may also be regarded as constant over a time required to accelerate particles from W_1 to the energies of interest, one finds the very useful result that over the energy range $W_2 < W < W_3(t)$, the shape of the energy is independent of time and of the detailed form of S. For W_a and W_b in this range,

$$\frac{n(W_a)}{n(W_b)} = \frac{W_a}{W_b} \left(\frac{W_a^{2} - 1}{W_b^{2} - 1} \right)^{\frac{1}{2 < \mu^2 >} - 1} \left\{ \frac{W_a + \sqrt{W_a^{2} - 1}}{W_b + \sqrt{W_b^{2} - 1}} \right\}^{-\frac{b}{a}} \tag{6}$$

and where $W_3(t)$ is given by

$$\frac{W_3^{\,2} - 1}{W_1^{\,2} - 1} = \left[\frac{L(t)}{L_0} \right]^{-2 <\mu^2>} . \tag{7}$$

There are, of course, no particles with energies below W_1. To facilitate comparison with observed spectra, we note that under the assumption that the pitch angle distribution is independent of energy the flux is proportional to $v_p n = c \sqrt{1 - \frac{1}{W^2}}\, n(W)$. Thus, if $F(W)$ is the flux at energy W, we have

$$\frac{F(W_a)}{F(W_b)} = \left(\frac{W_a^{\,2} - 1}{W_b^{\,2} - 1} \right)^{\frac{1}{2}\left[\frac{1}{<\mu^2>} - 1\right]} \left\{ \frac{W_a + \sqrt{W_a^{\,2} - 1}}{W_b + \sqrt{W_b^{\,2} - 1}} \right\}^{-\frac{b}{a}} . \tag{6^1}$$

Between $W_3(t)$ and $W_{max}(t)$, $n(W, t)$ decreases to zero in a manner dependent on S. Above $W_{max}(t)$, of course, $n(W, t)$ is zero. As $W_3(t)$ and $W_{max}(t)$ increase with time (or decreasing $L(t)$) we have a constantly lengthening region in which the spectrum is given by equation (6). This is a particularly interesting result if an essentially time independent $S(W, t)$ is sharply peaked in energy at $W \simeq W_2 \simeq W_1$. In this case equation (6) gives the (time independent) spectrum except for the constantly increasing cutoff at $W_{max}(t) \simeq W_3(t)$. This last assumption, although stringent, may be used to give a zeroth order approximation to the spectrum if $S(W, t)$ is not well known. In principle, observations at the cutoff energies would give the energy dependence of S, if it were time independent. In section III it is shown that the quasi-thermalized plasma behind the shock may provide an attractive source with the desired properties of time independence and a sharply peaked spectrum.

The assumptions introduced make the derived spectrum only approximate. The cutoff at $W_{max}(t)$ will be sharp only to the extent that it is improbable that a particle gain appreciably more or less than the average energy. It has been shown that the r. m. s. spread in energy is of the order of $\frac{1}{\sqrt{N}}$ W and may therefore be negligible if the number of cycles N is large. This is facilitated by a small fractional gain in energy per cycle and therefore may be a better approximation for electrons than protons at low energies.

Also, as stated above, the analysis breaks down when L(t) approaches r_g. The situation for $L(t) \lesssim r_g$ is difficult to analyse and we will confine attention to cases where $L_0 \gg r_g$ and L(t) only approaches r_g a negligible time before L(t) reaches zero. The main effect, then, is a limitation in the maximum energy attainable in a given event. This maximum energy $W_{L=0}$ can be roughly approximated by substituting $L(t) \simeq r_g = \frac{pc}{eB_0}$ in equation (5).

$$\left[W_{L=0}^2 - 1\right]^{(1 + <\mu^2>)} = \left[W_2^2 - 1\right]\left[\frac{L_0 e B_0}{m_0 c^2}\right]^{2<\mu^2>} . \tag{8}$$

This, although crude, should give a reasonable estimate of the allowed energies.

III. Sources of Particles to be Accelerated

Up till now the existence of particles that can be trapped and accelerated has been rather cavalierly assumed. It remains to determine the conditions under which a given particle may be accelerated and then to consider possible sources of eligible particles. The conditions that a particle must meet are that it have a reasonable probability of being reflected from the shock or the mirror and that the energy gains according to equation (1) offset the losses.

Consider first the reflection process. As discussed in Appendix 1, losses at the mirror begin to be large for particles whose velocities are not somewhat larger than $c\beta_0$. This effectively rules out the acceleration of thermal ions since $c\beta_0$ is of the order of the shock velocity relative to the plasma and is therefore likely to be greater than the mean thermal ion velocity. The acceleration of the bulk (or thermal) ions and electrons is also ruled out because they cannot be reflected at the shock front. For, reflection of an appreciable fraction of the plasma would not be consistent with the existence of a shock front. In the absence of detailed knowledge of the shock structure it is not possible to be more explicit and it will be assumed that particles (either ions or electrons) must satisfy both of the above mentioned general constraints to be efficiently accelerated. They must be both suprathermal and have velocities appreciably greater than $c\beta_0$. One may conclude that injection of electrons is favored over protons or other ions because at a given suprathermal energy the electrons will have a far greater velocity.

Collisional energy losses can be treated more explicitly. We consider only the situation in which the ambient plasma is fully ionized. First note that since we are interested in the injection of relatively low energy particles, it is reasonable to neglect synchrotron radiation and bremsstrahlung. The effects of these on relativistic particles is considered in the next paragraph. Since collisional losses in a fully ionized plasma decrease with increasing energy, it is sufficient to require that at $t = t_0$,

$$-\left(\frac{dW}{dt}\right)_{\text{collisions}} < \left(\frac{dW}{dt}\right)_{\text{acceleration at } t = t_0} \tag{9}$$

Spitzer (1956) gives the characteristic energy loss time for non-relativistic test particles as

$$t_E \simeq \frac{m_p^2 v_p^3}{32\pi e^4 z_1^2 z_p^2 n_1 \ell n \Lambda} \; \frac{1}{G\left(\sqrt{\frac{m_1 v_p^2}{2kT}}\right)} \tag{10}$$

where $G(X) = \frac{1}{X^2\sqrt{\pi}}\left[\int_0^X e^{-y^2} dy - Xe^{-X^2}\right]$ is tabulated by Spitzer (1956), $\ell n \Lambda$ is the usual coulomb logarithm and n_1, m_1, T refer to the field particles through which the test particle (m_p, v_p) is moving. Spitzer also notes that for $v_p >> \sqrt{\frac{2kT}{m_1}}$, $G\,\ell n\,\Lambda$ must be replaced by $0.5\left(1 + \frac{m_1}{m_p}\right)^{-2}$. Setting $\left(\frac{dW}{dt}\right)_{\text{collisions}} \simeq -\frac{E}{t_E}$ where $E = W - m_0c^2 << m_0c^2$ is the particle kinetic energy and using the non-relativistic limit of equation (1), equation (9) becomes

$$\frac{\beta_0 c < \mu^2 > m_p^2 v_p^3}{n_1 L_0} > 16\pi e^4 z_1^2 z_p^2 \, G\left(\sqrt{\frac{m_1 v_p^2}{2kT}}\right) \ln \Lambda . \qquad (11)$$

If the inequality in equation (11) is satisfied for a given group of test particles in the ambient plasma, and if they also satisfy the general conditions for reflection obtained in the preceding paragraph, they are then subject to acceleration as discussed in section 2.

As an example of the magnitudes involved, consider a typical shock traveling at 1000 km $\sec^{-1}$ through an ambient plasma at a temperature of 10^5 - 10^6 ^{o}K. It will accelerate 1 keV electrons if $n_1 L_0 \lesssim 10^{18} \text{cm}^{-2}$ and 1 keV protons if $n_1 L_0 \lesssim 10^{19}$ cm^{-2}. For nominal L_0 values of 10^{10} - 10^{12} cm, this is clearly not a serious restriction until densities approach coronal values of 10^7 cm^{-2}.

For completeness we briefly consider bremstrahlung and synchrotron radiation losses for relativistic electrons. If $W >> 1$, the losses for a particle in a proton-electron gas of density n_1 cm^{-3} and magnetic field intensity B can be written

$$-\frac{dW}{dt} = 1.37 \times 10^{-16} n_1 W \left\{ \ln\left(\frac{W}{m_0 c^2}\right) + 0.36 \right\} \text{ ergs sec}^{-1} \qquad \text{(Bremstrahlung)}$$

$$-\frac{dW}{dt} = 1.57 \times 10^{-15} B^2 \left(\frac{W}{m_0 c^2}\right)^2 \text{ ergs sec}^{-1} \qquad \text{(Synchrotron)}$$

where cgs units are used throughout. (See, e. g. Ginzburg and Syrovatsky, 1964). These are to be compared with the relativistic form of equation (1)

$$\frac{dW}{dt} = \beta_0 c \frac{\mu^2}{L(t)} W.$$

Putting in a nominal value of 1000 km sec^{-1} for the shock velocity $c\beta_0$, one finds that bremstrahlung and synchrotron radiation are unimportant unless, respectively, $n_1 L \gtrsim 10^{22} cm^{-2}$ for bremstrahlung and $L B^2 \frac{W}{m_0 c^2} \gtrsim 10^{16}$ cgs, synchrotron radiation. For most applications these limits are well satisfied.

It is clear that ambient energetic particles and a few supra-thermal plasma particles may satisfy the requirements and be accelerated, although they are not likely to be numerous except under special circumstances. A much more attractive source is the thermalized plasma behind the shock, some particles of which may escape to the front of the shock and be accelerated. If a plasma of mean particle mass $\overline{m}$ flows into the shock at velocity v_0 and leaves at v_1, energy conservation indicates that the mean increase in thermal energy per particle across the shock is of order $\Delta E \simeq f \frac{\overline{m}}{2} (v_0^2 - v_1^2)$, where f is a factor of order unity depending on the thermal degrees of freedom behind the shock and the form of equipartition. This expectation is supported by observations of keV electrons behind the earth's bow shock (Freeman, Van Allen and Cahill, 1963). For strong shocks in a relatively cold plasma, this represents an appreciable increase, particularly for electrons. This source is possibly not very efficient for the ions in the plasma since $\Delta E \simeq f \frac{\overline{m}}{2} (v_0^2 - v_1^2)$ may not be sufficient to make the ion velocity much greater than $c\beta_0 \simeq v_0$, as required for efficient reflection at the mirror. It is reasonable to conjecture that a fraction of these particles may escape along the magnetic field to the trapping region ahead of the shock, providing an S(W, t) that is very nearly time independent and which may be assumed to be peaked at a kinetic energy of the order of $\frac{\overline{m}}{2}(v_0^2 - v_1^2)$. The energy spectrum of energetic particles may therefore be well represented by equations (6) and (7). It will be found in the latter part of this paper that this source for electrons is strongly indicated for the earth's bow shock.

IV. Particles Behind the Shock

Having determined the spectrum in the trapping region, we proceed to consider the behavior of particles behind the shock. Since we are considering an essentially collisionless plasma, the details of the shock structure are not known. It is expected that the magnetic field in the region immediately behind the shock front is rapidly fluctuating and this expectation is confirmed by observations behind the earth's bow shock (Ness, Scearce and Seek, 1964). In such a turbulent field it is convenient to treat the average particle motion in the diffusion, or random walk, approximation with mean free path λ determined by the magnetic field structure. It will be assumed that λ is somewhat greater than the particle gyro-radius, in which case the motion is mainly along the average post shock magnetic field B_1, with a diffusion coefficient $K = \lambda v_p$. It should be noted that the qualitative nature of the conclusions will not be changed if this assumption is not correct. Attention is confined to that region behind the shock in which λ is constant. The field fluctuations may damp out a long distance behind the shock, but this will not be considered. Then the particle number density $\rho(t, \ell, W)dW/cm^3$, as a function of time, the distance ℓ along B_1 from the shock front ($\ell = 0$), and energy is obtained from the one-dimensional diffusion equation

$$\frac{\partial \rho}{\partial t} = + K \frac{\partial^2 \rho}{\partial \ell^2} - c\beta_1 \frac{\partial \rho}{\partial \ell} \tag{12}$$

where $c\beta_1$ is, in analogy with $c\beta_0$, the average velocity of the magnetic field irregularities behind the shock. The second term on the right side of (12) thus gives the effect of the convective motion of the scattering centers. The relative motion of the irregularities, which could give rise to further Fermi acceleration behind the shock, will be neglected in this treatment. Equation (12) is to be solved for $t > t_0$, $0 \leq \ell < \infty$, subject to the boundary conditions that $\rho(t_0, \ell, W) = 0$ and $\rho(t, 0, W)$ is equal to $\rho_t(W, t)$, the density in the trapping region as determined from equation (4). The last boundary condition would have to be modified slightly if the flux of trapped particles onto the shock front were less than the flux at $\ell = 0$ predicted by equation (12). This case is uninteresting because it means that the reflection coefficient of the shock is low and acceleration inefficient. The general solution to equation (12) is easily found by standard mathematical techniques, as discussed briefly in Appendix III. The present discussion is confined to a consideration of the general nature of the solutions.

As discussed in section II, conditions are usually such that there is a maximum energy at a given time which is given by equation (5). For any given W above the injection energy, therefore, $\rho(t, 0, W) = 0$ for $t < t_W$ where $W_{max}(t_W) = W$. Further, if the source function for injected particles is essentially constant and is peaked at $W = W_2$, then $\rho(t, 0, W)$ rises sharply at t_W to a constant value and remains there until the mirror is engulfed by the shock. The solution for this case is discussed in Appendix III. The particle diffusion velocity at $\ell = 0$ is shown to be

$$(v_D)_{\ell = 0} = \sqrt{K} \exp - \left[\frac{c^2\beta_1^2}{4K}(t - t_W)\right] \left\{\frac{1}{\sqrt{\pi}\sqrt{t - t_W}}\right.$$

$$\left. - \frac{c\beta_1}{2\sqrt{K}} \exp\left[\frac{c^2\beta_1^2}{4K}(t - t_W)\right] \operatorname{erfc}\left(\frac{c\beta_1}{2\sqrt{K}}\sqrt{t - t_W}\right)\right\} + c\beta_1 \quad (13)$$

Usually K is small enough so that the time for $(v_D)_{\ell = 0}$ to approach $c\beta_1$ is negligible. The flux is then mostly due to convection of particles with magnetic irregularities. Clearly this result is also true for any $\rho(t, 0, W)$ that does not change appreciably over the time it takes $\langle v_D \rangle_{\ell = 0}$ to become essentially equal to $c\beta_1$. The energy spectrum of the accelerated particles behind the shock should therefore, in the absence of rapid changes in $\rho(t, 0, W) = \rho_t(W, t)$, be essentially the same as in the trapping region. In addition, if $c\beta_1 \ll v_p(W)$, the trapped particle velocity, most of the particles incident on the shock front are reflected. The reflection coefficient of the shock can then be written

$$r_s \simeq 1 - \frac{c\beta_1}{v_p(W) \langle \mu^3 \rangle}, \quad (14)$$

where $< \mu^3 > = \frac{1}{4}$ for an isotropic distribution. We see that particles can be efficiently accelerated only if $c\beta_1 << v_p$ (W). Since ions are much slower than electrons at a given non-relativistic energy we again expect electrons to be accelerated more efficiently than protons or other ions.

At time $t_c = t_0 + \frac{L_0}{\beta_0 c}$, $L(t) = 0$ and the magnetic mirror is convected through the shock front. It accelerates no more particles and $\rho_t \simeq 0$ for $t > t_c$. This will, of course, affect the structure of the shock, but this may not be important. If the effects on the shock are neglected, we can treat the behavior of the particles as above except that the boundary condition at $\ell = 0$ becomes $\rho(t, 0, W) \cong 0$ for $t > t_c$. This is again a well defined mathematical problem and can be treated by the techniques of Appendix III. The particles stay on the same line of force, but now escape slowly from the end at $\ell = 0$. Since the diffusion coefficient is $K = \lambda v$, it is expected that the decay of the intensity is faster for more energetic particles.

The density of particles along the line of force at a given energy is schematically depicted in Figure 1 at two different times, $t_W < t < t_c$ and $t_c < t$, where it should be remembered that the intensity is zero everywhere for $t < t_W$.

It has been demonstrated that the irregular magnetic fields behind the shock dramatically reduce the flux of particles through the shock front, causing the shock front to have effectively unity reflectivity. However, that fraction of particles which penetrates the shock may gain more or less energy than that which is reflected at the shock. There are two reasons for this. The particles will take longer to complete a cycle; and the irregularities behind the shock may be moving. The first of these effects is probably small

Figure 1

A schematic sketch of the variation of ρ along a given field line for energy W at two different times. As discussed in the text, $\rho = 0$ for $t < t_W$. 1. a. indicates the behavior of ρ for a time t such that $t > t_W$, but the mirror is still some distance from the shock. As indicated by the heavy arrow, particles have begun to move into the region behind the shock by a combination of diffusion and convection. 1. b. shows the situation for a time $t > t_c$ so that the mirror has been absorbed by the shock. Particles now diffuse in both directions in addition to being convected by the magnetic irregularities.

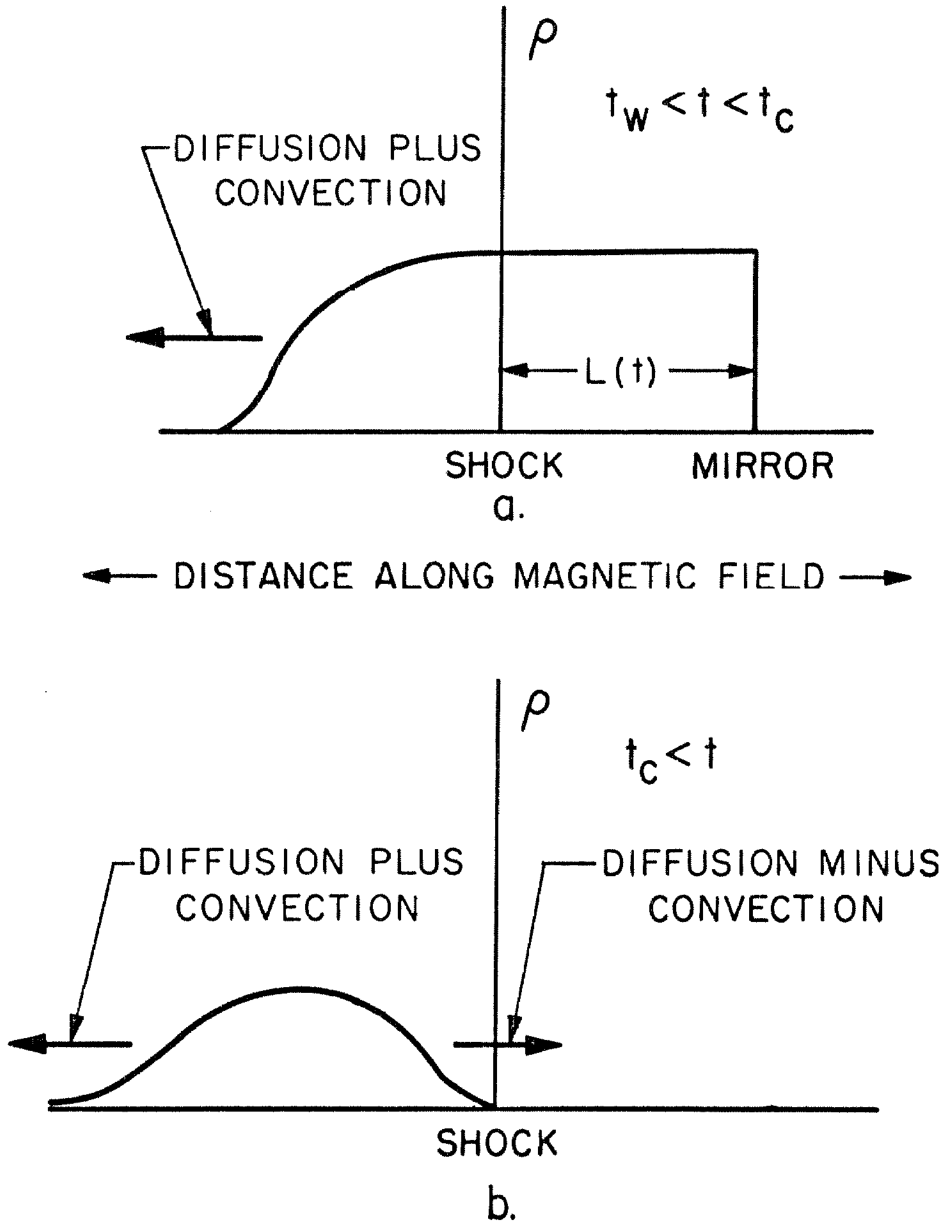
ρ
$t_W < t < t_C$
DIFFUSION PLUS CONVECTION
L (t)
SHOCK
MIRROR
a.
DISTANCE ALONG MAGNETIC FIELD
ρ
$t_C < t$
DIFFUSION PLUS CONVECTION
DIFFUSION MINUS CONVECTION
SHOCK
b.

Figure 1

since the mean depth of penetration into the region behind the shock is of the order of a few times λ and will be assumed to be much less than L(t).

The second effect is more important and may make the model relatively inefficient for weak shocks. The importance of the effect may be estimated as follows. The fraction of particles that are reflected at the shock is about $r_s \simeq 1 - B_0/B_1$ since for an isotropic pitch angle distribution this is independent of the conservation of magnetic moments (Wentzel, 1963). For these particles, the energy gain is given by equation (1). It is readily determined that the remainder of the particles gain more or less by the factor $(\beta_0 - \beta_1)/\beta_0$. A measure of the efficiency of the shock is then

$$q = 1 + \frac{\beta_1}{\beta_0}(r_s - 1) \tag{15}$$

which may approach unity for a strong shock and be nearly 0 for a weak shock. We will restrict our attention to strong shocks where the efficiency may be taken to be unity.

V. Limitations on Particle Density

One might inquire about collective effects of the accelerated particles. In the development of the model, single particle behavior has been assumed and this clearly limits the density of accelerated particles. A reasonable criterion for the validity of the model is that the trapped particle kinetic energy density be substantially less than that of the magnetic field. That is

$$\int_1^\infty \rho_t(W)[W - 1]dW < \frac{B_0^2}{4\pi m_0 c^2} \quad . \tag{16}$$

If equation (16) is not satisfied, the collective behavior of the particles becomes important and the model is not applicable. The process of acceleration would then itself modify the ambient magnetic field configuration and perhaps the shock structure.

This depends on the value of the parameters for each case. Clearly if X were nearly zero, the spectrum would be quite flat and equation (16) may not be satisfied. Under most conditions, however, the spectrum will be sufficiently steep so that equation (16) is satisfied.

Applications

VI. Interpretation of Electron Pulses Observed Beyond the Magnetosphere

The theory of Fermi acceleration described above will now be applied to electrons at the earth's bow shock. Recent observations of energetic electron pulses beyond the magnetosphere are first reviewed. It is shown that the most probable interpretation of the observations is in terms of the transient presence of electrons in an extended region of the transition region between the bow shock and the magnetopause. It is then noted that the presence of electrons beyond the bow shock and their apparent confinement to a narrow region beyond suggest the presence of magnetic irregularities beyond the shock. We are thus naturally led to an application of the ideas of the model discussed above. It is found that the model leads to a compelling quantitative understanding of most features of the phenomenon. A detailed explanation of the energetic electron events observed in the vicinity of the geomagnetic tail will not be attempted here.

The observations under consideration consist of pulses of $\gtrsim$ 30 keV electrons which are observed beyond the magnetosphere and, at times, beyond the earth's bow shock. They consist typically of fluxes of about $10^5 cm^{-2} sec^{-2}$ (> 30 keV), or about 10 times background, which last only a few minutes at the satellite and are extremely variable in magnitude and location. The short duration of the pulses indicates that they are of local origin and are probably accelerated in or near the magnetosphere of the earth. The pulses were first seen by Van Allen and Frank (1959). Observations by Fan, Gloeckler and Simpson (1964) and Anderson, Harris and Paoli (1964) using IMP-1 have done much to reveal their relationship to the magnetosphere and to the bow shock. Comparison with the IMP-1 magnetometer and plasma data as shown in Figure 2, show that the electron pulses occur beyond the bow shock, although they tend strongly not to be found more than a few earth radii beyond it. In addition, between the bow shock and the magnetopause, the pulses were observed much more often when far from the subsolar point than when near it. Anderson, Harris and Paoli (1964) report further that the pulses tend to more intense and more frequent near the magnetosphere. Frank and Van Allen (1964) have recently reported similar observations on Explorer XIV. They find the occurrence of the pulses to be positively correlated with k_p and report measurable fluxes of 1.6 MEV electrons (of the order of $10\ cm^{-2} sec^{-1}$ > 1.6 MEV).

Figure 2

A plot showing a direct comparison of IMP-1 magnetometer, interplanetary plasma and high energy (> 30 keV) electron data for the first nineteen imbound orbits. The hammers indicate the position of the earth's bow shock as determined from the magnetometer data (Ness *et al.*, 1964) and the plasma probe (Bridge *et al.*, 1964). The circles indicate the position of the outermost electron pulse observed on each orbit by Fan, Gloeckler and Simpson (1964). Note that the plasma and magnetometer data agree well on the location of the shock, but that the outermost electrons tend to occur somewhat beyond the shock. The electrons also tend strongly not to be found more than a few earth radii beyond the shock.

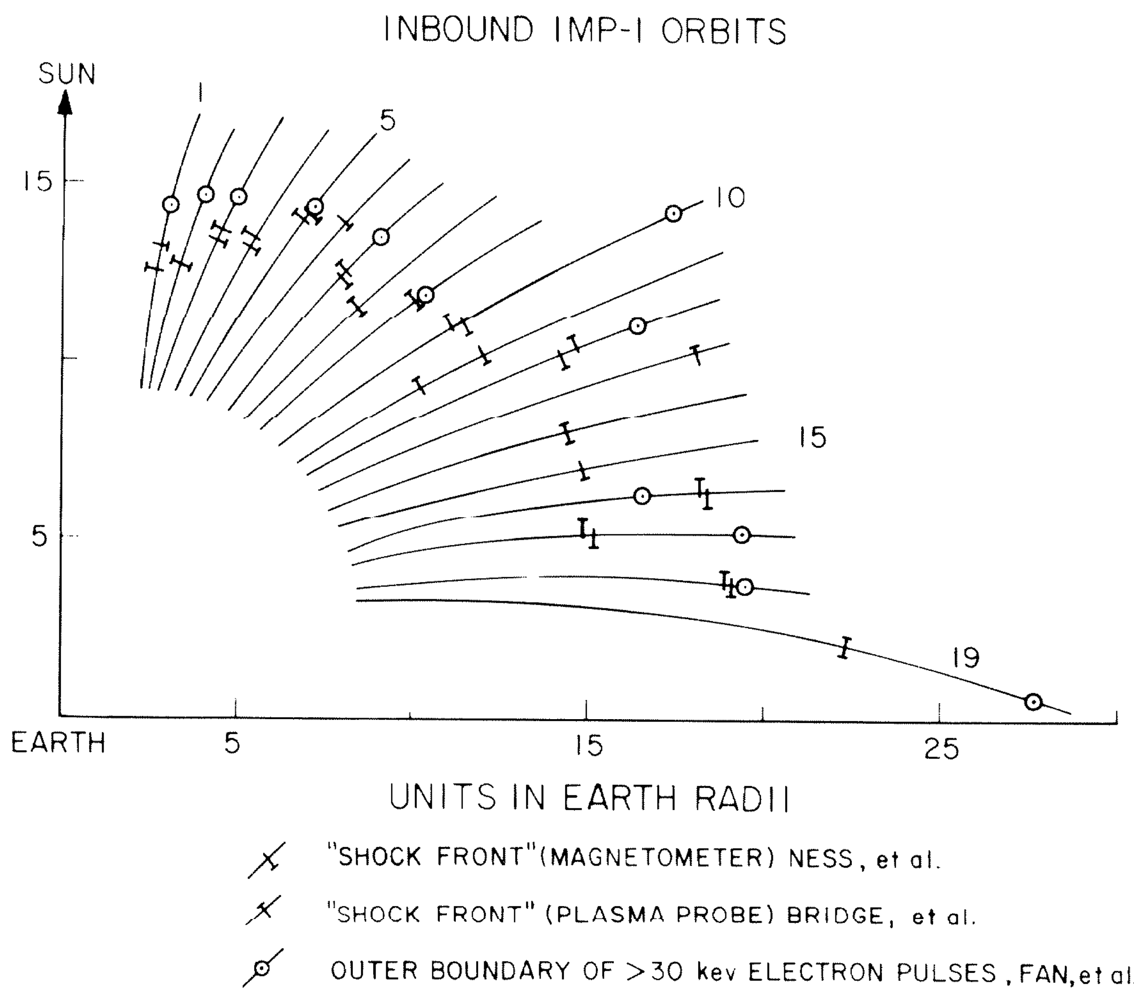
INBOUND IMP-I ORBITS
SUN
15
5
1
5
10
15
19
EARTH
5
15
25
UNITS IN EARTH RADII
"SHOCK FRONT"(MAGNETOMETER) NESS, et al.
"SHOCK FRONT" (PLASMA PROBE) BRIDGE, et al.
OUTER BOUNDARY OF >30 kev ELECTRON PULSES, FAN, et al.

Figure 2

More recently, detailed measurements of integral spectra of electrons in the energy range 50 keV $< E <$ 325 keV, together with their spatial and temporal variations at $R \simeq 17\ R_e$, have been reported by Montgomery, Singer, Conner and Stogsdill (1965). Their observations near the bow shock and in the transition region are apparently consistent with the earlier observations. They report a striking asymmetry in the occurrence of events between the dawn and evening sides of the magnetosphere, the pulses being appreciably more numerous on the dawn side.

They also report events on the night side of the magnetosphere, in the vicinity of the magnetospheric tail, which apparently last for several hours.

How are the electron pulses to be interpreted? Observations alone cannot answer this conclusively since one is faced with the usual ambiguity between spatial and temporal variations inherent in observations from a single, moving satellite. The extreme variability of the observed pulses argues against their being due to permanent belts of energetic electrons. There are, furthermore, compelling theoretical arguments against interpreting the pulses as due to the presence of electrons in localized regions of space, through which the satellite passes in a few minutes. Any energetic electrons must drift through the magnetic field with the bulk velocity of the solar wind, at about 400 km/sec. They also tend to spiral rapidly, about 10^{10} cm/sec, along the lines of force. Thus, if a localized source acts for more than a few tens of seconds, the flux must be appreciable in an extended region much larger than the 2,000 km that a satellite can traverse in a few minutes. It is suggested, therefore, that the pulses are due to the transient presence of electrons in an extended region, as in Figure 3. The duration of

Figure 3

Schematic representation. This indicates the suggested general interpretation of a pulse. Acceleration occurs somewhere in the region NABCN or perhaps in the magnetosphere. Boundaries NAD and NCF may not be sharp due to motion of particles along field lines. N can occur at various distances from S, the subsolar point. The solar wind blows accelerated particles into the region ABCFD and beyond. When trapping or acceleration ceases, the whole region drifts downwind.

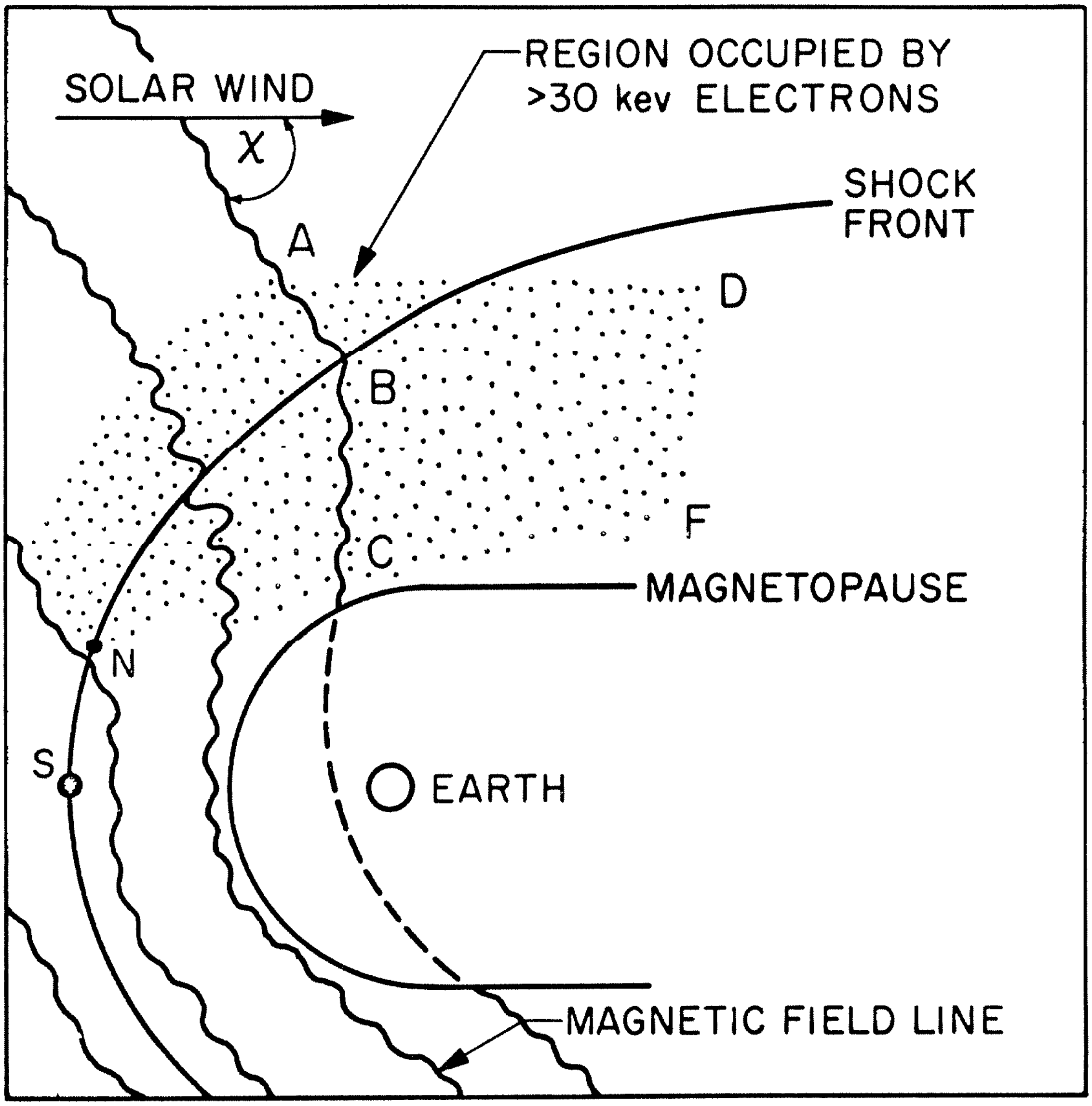
REGION OCCUPIED BY
>30 kev ELECTRONS
SOLAR WIND
χ
A
SHOCK
FRONT
D
B
F
C
MAGNETOPAUSE
N
S
EARTH
MAGNETIC FIELD LINE

Figure 3

their presence is that of the observed pulses and the region typically encompasses much of the transition region between the bow shock and the magnetopause. The motion of the electrons in the transition region will be, as discussed in section IV of this paper, essentially convection with the plasma together with a relatively slow diffusion along the field. Since more pulses were observed in the transition region when far from the subsolar point than when near it, it is reasonable that the region of electrons may, on different occasions, have its upwind edge at various distances from the subsolar point. The solar wind extends these regions downwind into the transition region. More regions would therefore be likely to sweep past the satellite when far from the subsolar point than when near it, explaining the frequency of pulses away from the subsolar point. Similarly the tendency for pulses to be more intense and numerous near the magnetopause may be a result of the flow around the magnetosphere and the associated deflection and compression of the plasma and magnetic field lines near the magnetopause.

VII. The Acceleration of Electrons at the Bow Shock

Within the above general interpretation of the pulses, it remains to determine the source of the electrons. Several possibilities have been suggested, although detailed models are lacking. It has been proposed that the electrons are of magnetospheric origin (Anderson, Harris and Paoli, 1964), or that they are heated by plasma instabilities in the transition region (Fredricks, Scarf and Bernstein, 1965).

First note that, whatever their source, the energetic electrons must be able to penetrate to the region in front of the shock. The observed cutoff in the pulses at a few times 10^9 cm in front of the shock indicates the presence of magnetic irregularities which reflect the electrons back toward the shock. Since these irregularities probably move relative to the shock (they are probably carried with the solar wind, which has a velocity several times the Alfvén velocity), we are led to the possibility that the particles are accelerated by a Fermi mechanism, and that perhaps most of the acceleration is accomplished in this manner.

We are thus naturally led to the hypothesis that each pulse of electrons is caused by one or more magnetic irregularities approaching the bow shock. The motion of particles behind the shock has already been discussed, and it is clear that the motion is consistent with the hypothesis. The remainder of this paper is devoted to demonstrating that the whole phenomenon can be quantitatively explained by this model. Note that the low ambient density in the solar wind makes it unnecessary to worry about collisional energy losses.

The bow shock is expected to heat particles to energies of the order of $\frac{\bar{m}}{2}(v_0^2 - v_1^2)$, or about 1 keV for a solar wind velocity of 500 km/sec. The existence behind the bow shock of electrons in this energy range is supported by observations of Freeman, Van Allen and Cahill (1963). Consider now the following sequence of events for the general configuration of Figure 3 . A field line, moving with the solar wind, has a magnetic irregularity B_M upwind from the bow shock. At time t_0 this field line connects with the shock and a small fraction of the ~ 1 keV electrons found behind the shock begin escaping along the field toward B_M and are subsequently accelerated as discussed previously. For simplicity we make the approximations that the bow shock is essentially plane and that the injected electrons are sharply peaked at about 1 keV. The spectrum is then given by equations (6) and (7), with a $W_1 \sim W_0 \sim 1$ keV and $\frac{b}{a}$ determined by the solar wind conditions. The bow shock is a strong shock, so q in equation (15) will be taken to be essentially unity.

Putting in characteristic dimensions and noting that the interplanetary magnetic field is usually inclined at about 45° to the wind velocity (Ness, Scearce and Seek, 1964), one finds that a typical L_0 should be of the order of a few times 10^{10} cm, or a characteristic dimension of the shock surface. Setting $W_1 \simeq W_0 \simeq$ keV and using equation (7), one finds that $W_{max}(t) = 30 \text{ keV} + m_0c^2$ (i. e. 30 keV electrons are first produced) corresponds to L(t) of the order of 10^9 cm, or a few R_E. Thus, pulses of 30 keV or higher electrons would tend not to be seen more than a few earth radii beyond the bow shock, in excellent agreement with the observed cutoff in > 30 keV pulses. Similarly, the duration of > 30 keV pulses should be of the order of the time required for the mirror, traveling at the solar wind velocity of 500 km/sec, to traverse this distance of a few R_E, or the observed few minutes. Note that it follows from equation (8) that for such an event and a 5γ magnetic field, the maximum energy $W_{L=0}$ is of the order of MeV. Also in gratifying agreement with observation is the expectation that, since the interplanetary magnetic field is preferentially inclined toward the dawn side of the magnetosphere as in Figure 3, the pulses should occur preferentially on the dawn side of the magnetosphere.

The average, statistical features of the observed pulses are thus shown to be in remarkable agreement with the Fermi acceleration hypothesis. That aspect of a single pulse most accessible to measurement is its energy spectrum. The excellent agreement between theory and observations is found below to extend to the details of the energy spectra.

According to the discussion in section IV, the predicted energy spectra during the main phase of an event should be the same in the transition region as in the trapping region. Before a detailed comparison with the data can be made, two parameters - the flux at some energy and the ratio $\frac{b}{a}$ - must be determined. Either or both vary considerably and depend on as yet unknown parameters of the solar wind and interplanetary magnetic field. In view of this it is most feasible to make a two parameter fit to the spectrum in each case and then determine whether the required parameters are reasonable. This was done for three integral electron spectra reported by Montgomery et al. (1965) which were taken at different times during the relatively constant phase of an event. The reported location of the observations, ecliptic latitude -5°, longitude 249°, magnetic latitude 11°, indicate that they were made in the transition region. The present model should therefore be applicable. Figure 4 displays the results. The dots with error bars are the observed points and the solid lines are two parameter fits to the observations. The predicted integral spectra were obtained from equation (6^1) by a three point Gaussian integration. It was assumed that the spectrum (6^1) extended to $W = \infty$ in the integrations. The steepness of the spectrum makes this reasonable. Because the function is very smooth and well behaved, it is believed that errors in this integration procedure are negligible. The curves are rather insensitive to variations in $< \mu^2 >$ and the isotropic value of $\frac{1}{3}$ was used.

Figure 4

The dots with error bars indicate 3 integral spectra reported by Montgomery et al. (1965). The spectra were obtained at 3 different times during the relatively constant phase of an event located at ecliptic latitude -5^{o}, ecliptic longitude 249^{o} and magnetic latitude 11^{o}. This is probably in the transition region on the morning side of the magnetosphere. The solid lines are theoretical fits to the data. The values of $\frac{b}{a}$ required to fit the curves are: for curve 1, $\frac{b}{a} = 18$; for curve 2, $\frac{b}{a} = 16.5$; and for curve 3, $\frac{b}{a} = 22.3$.

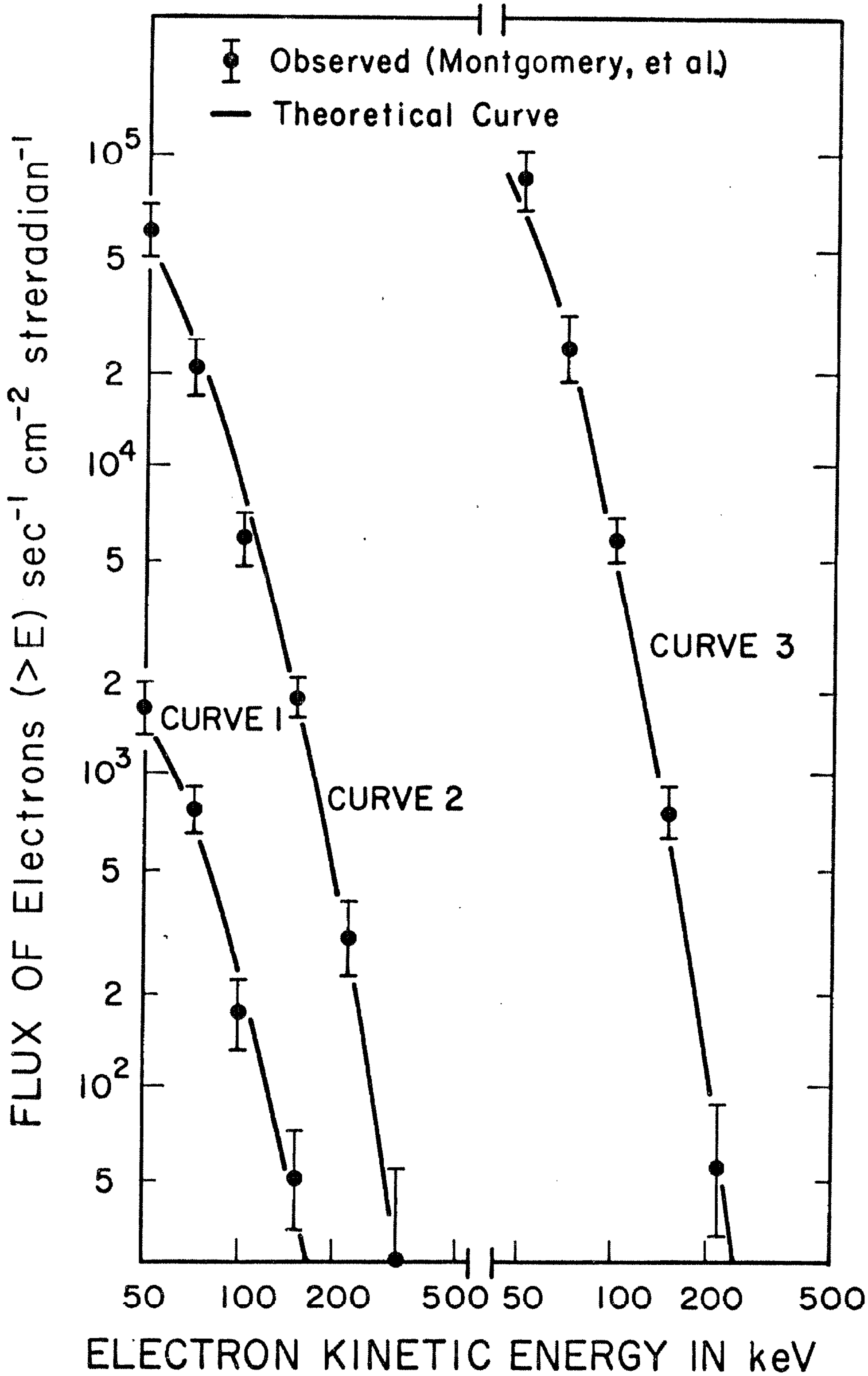
Observed (Montgomery, et al.)
Theoretical Curve
FLUX OF Electrons (> E) sec⁻¹ cm⁻² streradian⁻¹
10⁵
5
2
10⁴
5
2
10³
5
2
10²
5
CURVE 1
CURVE 2
CURVE 3
50
100
200
500
50
100
200
500
ELECTRON KINETIC ENERGY IN keV

Figure 4

The agreement is clearly excellent and is much better than a straight line, or power law, fit. That the shapes of the spectra are in so close agreement indicates that the agreement is meaningful in spite of there being two adjustable parameters.

In addition, Frank and Van Allen (1965) have reported a partial spectrum for one pulse. They find integral fluxes of $\simeq 10^6$ cm^{-2}sec^{-1} at $E > 40$ keV; $\simeq 30$ cm^{-2}sec^{-1} at $E > 1.6$ MeV and an upper bound of about 10^4 cm^{-2}sec^{-1} at $E > 230$ keV. These are consistent with a value of about 12 for $\frac{b}{a}$. The spectrum was therefore somewhat harder (less steep) in this event. Since a harder spectrum corresponds to a larger wind velocity or a larger mirror ratio, it is reasonable that this pulse was unusually intense and occurred on a day with a high k_p index.

Are the required parameters reasonable? The required flux of injected electrons $\gtrsim 1$ keV is of the order of 10^6 cm^{-2}sec^{-1} in each case, so that only about 1% of the approximately 3×10^8 electrons cm^{-2}sec^{-1} incident on the shock need escape to be accelerated. The required values of $\frac{b}{a}$ are not very different as would be expected for the same event. The slight difference may be due to some small effect such as the curvature of the shock, or some fluctuation during the acceleration. To show that values for $\frac{b}{a}$ in the range 15 - 20 are consistent with our knowledge of the solar wind, more analysis is necessary.

Note first that the solar wind is usually inclined at an angle to the interplanetary field, as indicated schematically in Figure 3. In order to obtain an estimate for $c\beta_0$, we must transform to a frame in which the shock is stationary and the solar wind velocity is either parallel or anti-parallel to the interplanetary magnetic field. In the limit that β_0^2 can be neglected compared to unity this transformation does not change the magnetic field and so is simple to carry out. As shown in Appendix IV, one obtains, in terms of $\underset{\sim}{v}_W$ the wind velocity, the angle χ between $\underset{\sim}{B}_0$ and $\underset{\sim}{v}_W$ ($\cos\chi = -(\underset{\sim}{B}_0 \cdot \underset{\sim}{v}_W)(\underset{\sim}{B}_0 \cdot \underset{\sim}{n})/B_0 v_W |\underset{\sim}{B}_0 \cdot \underset{\sim}{v}_W|$), and the angle α between $\underset{\sim}{n}$, the shock normal and $\underset{\sim}{v}_W$ ($\cos\alpha = \pm\, \underset{\sim}{v}_W \cdot \underset{\sim}{n}/v_W$, the sign of α being the sign of $|\underset{\sim}{B}_0 \cdot \underset{\sim}{n}| - |\underset{\sim}{B}_0 \cdot \frac{\underset{\sim}{v}_W}{v_W}|$),

$$c\beta_0 = \frac{v_W}{\cos\chi} \left[\frac{1}{1 + \sin\alpha \tan\chi} \right] . \qquad (17)$$

Assuming a nominal wind velocity of 500 km sec^{-1} and setting $\chi = 45^{\circ}$, the average spiral angle of the interplanetary magnetic field, we find $\beta_0 \simeq 2.5 \times 10^{-3}$ for $\alpha \simeq 0$ which corresponds to the subsolar point. Away from the subsolar point α increases slowly and β_0 decreases slightly as the mirror approaches the shock. For an isotropic pitch angle distribution $<\mu> \simeq \frac{1}{2}$, $<\mu^2> \simeq \frac{1}{3}$ and $\frac{b}{a} \simeq 0.3 \times 10^3$ X. Therefore values of $\frac{b}{a}$ in the range 15 to 20 require that X be about 0.05 - 0.10. Setting $X_i = 0.05 - 0.10$ suggests that B_M/B_0 must be about 7 to 10, but this is probably only an upper limit on the required mirror ratio. Because Frank and Van Allen find the pulses to be correlated with k_p and therefore perhaps with v_W (Snyder, Neugebauer and Rao, 1963), these estimates based on quiet day solar wind parameters may be conservative.

We find, therefore, that the proposed model of Fermi acceleration is in excellent quantitative agreement with the electron pulses observed near the earth's bow shock. It is expected that protons should also be accelerated, although because of their larger gyro-radii and lower velocities they should be accelerated less efficiently. Evidence for proton events has been reported (Montgomery *et al.*, 1965).

Further observations are desirable to further test predictions of this model. Analysis of simultaneous energetic particle and magnetic field measurements, both in the transition region and beyond the bow shock would help to determine the magnetic field configurations associated with the particles. Detailed energy spectra are, of course, essential. A very useful test of the Fermi acceleration hypothesis would be an analysis of the variation of the cutoff distance from the bow shock as a function of energy. Confirmation of this effect would be strong support for this model.

Appendix

I. Reflection of a Particle by a Moving Magnetic Mirror

We first consider reflection from a stationary magnetic mirror with the intention of later transforming to a frame in which the mirror has a velocity $c\beta_0$. Suppose a particle to be moving in a uniform magnetic field $\underset{\sim}{B}_0$ toward a region of increasing field with maximum intensity $B_M = s\,B_0$, where $\underset{\sim}{B}_M$ is parallel to $\underset{\sim}{B}_0$. The restriction to $\underset{\sim}{B}_M$ and $\underset{\sim}{B}_0$ parallel will be shown to be unnecessary if β_0^2 can be neglected compared to unity. If $P_\parallel^*$ and $P_\perp^*$ are, respectively, the momenta of the particle parallel and perpendicular to $\underset{\sim}{B}_0$, the condition that the particle's magnetic moment $\left(\frac{P_\perp^2}{B}\right)$ be an invariant yields the familiar reflection criterion:

$$\frac{(P_\perp^*)^2}{B_0} > \frac{P_\perp^{*2} + P_\parallel^{*2}}{B_M} = \frac{P^{*2}}{B_M} \qquad \text{(I-1)}$$

or, defining $\mu_0^* = \frac{P_\parallel^*}{P^*}$,

$$\mu_0 < \sqrt{1 - \frac{1}{s}} \ . \qquad \text{(I-2)}$$

Now make a Lorentz transformation to a frame in which the mirror moves with velocity $v = c\beta_0$ parallel to $\underset{\sim}{B}_0$ toward the particle. If unstarred symbols designate the parameters in this frame, we find

$$P_\perp^* = P_\perp \text{ and } P_\parallel^* = \gamma_0(P_\parallel + \beta_0 \frac{W}{c}) \tag{I-3}$$

and $\underset{\sim}{B}_0$ and $\underset{\sim}{B}_M$ remain unchanged, where $\gamma_0^2 = \frac{1}{1 - \beta_0^2}$ and W is the total partical energy. Substituting these into equation (I-1) yields

$$s - 1 \geq \left(\frac{P_\parallel^*}{P^*}\right)^2 = \frac{\left(\mu_0 + \beta_0\sqrt{1 + \frac{m_0^2c^2}{P^2}}\right)^2}{(1 - \mu_0^2)(1 - \beta_0^2)} \;. \tag{I-4}$$

It is then apparent that any particle with $\mu_0 < \mu_c$ is reflected by the moving mirror, where μ_c satisfies

$$\frac{(1 - \mu_c^2)(1 - \beta_0^2)}{\left[\mu_c + \beta_0\sqrt{1 + \frac{m_0^2c^2}{P^2}}\right]^2} = \frac{1}{s - 1} \;. \tag{I-5}$$

Since changes in magnetic field intensities under Lorentz transformations are of order β_0^2 compared to 1, the restriction to $\underset{\sim}{B}_0$ being parallel to $\underset{\sim}{B}_M$ can be relaxed if β_0^2 is negligible compared to 1. This is true in most cases of practical interest.

Once μ_c is known, the transmission factor of the mirror for a known distribution of pitch angles can be calculated.

$$X = \frac{\int_0^{\cos^{-1}\mu_c} n(\theta)d\theta}{\int_0^{\pi/2} n(\theta)d\theta} \quad . \tag{I-6}$$

If the distribution is isotropic, $n(\theta)d\theta = A \sin\theta d\theta$ and

$$X_i = 1 - \mu_c \quad . \tag{I-7}$$

If the pitch angle distribution is isotropic, in the limit $v_p \gg c\beta_0$, one finds the familiar result

$$X_i \simeq 1 - \sqrt{1 - B_0/B_M} \, . \tag{I-8}$$

But, if $v_p \lesssim c\beta_0$, μ_c becomes small and X_i approaches unity.

The energy gain of a reflected particle is also readily calculated. Note first that in the rest frame of the mirror the energy and perpendicular momentum of the particle are unchanged, but that the parallel momentum is reversed. A particle having an initial energy W_i and parallel momentum $(P_{\parallel})_i$ will have $W^* = \gamma_0[W_i + \beta_0 c(P_{\parallel})_i]$ and $P_{\parallel}^* = \gamma_0[(P_{\parallel})_i + \beta_0 \frac{W_i}{c}]$ in the rest frame of the mirror. Reversing $P_{\parallel}^*$ and transforming back to the original coordinate system, one readily obtains

$$(W_f - W_i) = \Delta W \simeq 2\gamma_0^2 \beta_0 [(cP_{\parallel})_i + \beta_0 W_i] \, . \tag{I-9}$$

If the particle makes $\frac{\mu v_p}{2L(t)}$ reflections per second, where $2L(t)$ is the distance travelled between reflections, the rate of energy gain can be written

$$\frac{dW}{dt} \simeq \frac{1}{1 - \beta_0^2} \left[\frac{\mu^2 c \beta_0}{L(t)} W \left(1 - \frac{m_0^2 c^4}{W^2}\right)\right]\left[1 + \frac{\beta_0}{\mu\beta_p}\right] \qquad \text{(I-10)}$$

where $\beta_p = \frac{v_p}{c} = \left(1 - \frac{m_0^2 c^4}{W^2}\right)^{\frac{1}{2}}$. We are chiefly interested in the limit $\beta_0/\beta_p \ll 1$ and $\beta_0^2 \ll 1$, so that

$$\frac{dW}{dt} \simeq \frac{\mu^2 c \beta_0}{L(t)} W \left(1 - \frac{m_0^2 c^4}{W^2}\right) . \qquad \text{(I-11)}$$

II. Solution of the Particle Conservation Equation

A formal Green's function solution to equation (3) is readily obtained. First, define a new time variable $\psi = \psi_0 - \frac{1}{\beta_0 c} \ln \left[\frac{L(t)}{L_0(t_0)} \right]$. Then equation (3) can be written

$$\frac{\partial n}{\partial \psi} + aW\left(1 - \frac{1}{W^2}\right)\frac{\partial n}{\partial W} + \left[b\sqrt{1 - \frac{1}{W^2}} + a\left(1 + \frac{1}{W^2}\right)\right] n = S^*(W, \psi) \qquad \text{(II-1)}$$

where W is written in units of m_0c^2 and $S^*(W, \psi) = L(t(\psi))\, S(W, t(\psi))$, where the above equation for ψ is easily inverted to give $t(\psi)$. Equation (II-1) is to be solved for $\psi > \psi_0$, $W > 1$ subject to the boundary conditions that $n(W, \psi_0) = n(1, \psi) = 0$. Replacing $S^*(W, \psi)$ by $\delta(W - W_1)\, \delta(\psi - \psi_1)$ in equation (II-1) and solving by the Laplace transform technique, one eventually obtains the Green's function for equation (II-1),

$$n_g(W, \psi; W_1, \psi_1) = \theta(W - W_1)\, \delta\left(\psi - \psi_1 - \frac{1}{2a} \ln \frac{W^2 - 1}{W_1^2 - 1}\right) \times$$

$$\times \frac{W}{a(W^2 - 1)} \left[\frac{W + \sqrt{W^2 - 1}}{W_1 + \sqrt{W_1^{\,2} - 1}}\right]^{-\frac{b}{a}} . \qquad \text{(II-2)}$$

The general solution to equation (II-1) is then

$$n(W, \psi) = \int_1^{\infty} dW_1 \int_{\psi_0}^{\infty} d\psi_1 \, [n_g(W, \psi; W_1, \psi_1)] \, S_*(W_1, \psi_1) \qquad \text{(II-3)}$$

The ψ_1 integral is trivial; one obtains

$$n(W, \psi) = \frac{W(W + \sqrt{W^2 - 1})^{-\frac{b}{a}}}{a(W^2 - 1)} \int_1^{\infty} dW_1 \, \theta(W - W_1) \, \theta\left(\psi - \psi_0 - \frac{1}{2a} \ell n \frac{W^2 - 1}{W_1^2 - 1}\right)(W_1 + \sqrt{W_1^2 - 1})^{\frac{b}{a}}$$

$$S_*\left(W_1, \psi - \frac{1}{2a} \ell n \frac{W^2 - 1}{W_1^2 - 1}\right) dW_1 \qquad \text{(II-4)}$$

or,

$$n(W, t) = \frac{W(W + \sqrt{W^2 - 1})^{-\frac{b}{a}} L(t)}{a(W^2 - 1)^{\left(1 - \frac{1}{2 < \mu^2 >}\right)}} \int_1^{\infty} dW_1 \, \theta(W - W_1)$$

$$\frac{(W_1 + \sqrt{W_1^2 - 1})^{\frac{b}{a}}}{(W_1^2 - 1)^{\frac{1}{2 < \mu^2 >}}} \, S(W_1, t^1) \, \theta\left[\left(\frac{L(t)}{L_0}\right)^{-2 < \mu^2 >} - \frac{W^2 - 1}{W_1^2 - 1}\right] \qquad \text{(II-5)}$$

where $$t^1 = \frac{L_0}{\beta_0 c} + \left(t - t_0 - \frac{L_0}{\beta_0 c}\right)\left(\frac{W^2 - 1}{W_1^2 - 1}\right)^{\frac{1}{2 < \mu^2 >}} + t_0 \, .$$

In spite of the complexity, some useful limiting results may be drawn from equation (II-5) as is discussed in the text.

III. The Diffusion Equation with Convection of Scattering Centers

Equation (12) is to be solved for $\rho(\ell, t, W)$ subject to the boundary conditions that $\rho(\ell, 0, W) = 0$ and $\rho(0, t, W) = g(t, W)$ is a known function. The general solution is easily found by standard Laplace transform methods, and only the final result for the general case is present. One obtains

$$\rho(\ell, t, W) = \mathcal{L}_s^{-1}[F(\ell, s, W)] \tag{III-1}$$

where $\mathcal{L}_s^{-1}(f)$ is the inverse Laplace transform of f and where

$$F(\ell, s, W) = \exp\left\{\left[\frac{c\beta_0}{2K} - \sqrt{\frac{c^2\beta_1^2}{4K^2} + \frac{s}{K}}\right]\ell\right\}\int_0^\infty g(t, W)e^{-st}dt. \tag{III-2}$$

For the special case discussed in the text where $g(t, W)$ can be expressed as $\rho_0(W)\,\theta(t)$, then

$$\rho(\ell, t, W) = \rho_0(W)\left\{1 - \frac{2}{\pi}\exp\left[\frac{c\beta_1\ell}{2K} - \frac{c^2\beta_1^2}{4K}t\right]\int_0^\infty \frac{z^2}{z^2 + \frac{c^2\beta_1^2}{4K}}\sin\frac{\ell}{\sqrt{K}}z\, e^{-tz^2}dz\right. . \tag{III-3}$$

A quantity of interest, the average velocity at $\ell = 0$ is obtainable in terms of familiar functions. Setting

$$\langle v_D \rangle_{\ell = 0} = c\beta_1 - K \left(\frac{\partial \rho}{\partial \ell}\right)_{\ell = 0} \cdot \frac{1}{\rho_0} \;, \qquad \text{(III-4)}$$

one obtains

$$\langle v_D \rangle_{\ell = 0} = \sqrt{K} \exp - \left(\frac{c^2\beta_1^2 t}{4K}\right) \left[\frac{1}{(\pi t)^{1/2}} - \frac{c\beta_1}{2\sqrt{K}} \exp \frac{c^2\beta_1^2 t}{4K} \operatorname{erfc}\left(\frac{c\beta_1}{2\sqrt{K}}\sqrt{t}\right)\right]$$

$$+ \; c\beta_1 \qquad \text{(III-5)}$$

Clearly, as $\frac{K}{c^2\beta_1^2 t} < 1$, this rapidly approaches $c\beta_1$.

IV. Transformation to the "Preferred" Reference System for a Point on the Earth's Bow Shock

If the magnetic field has a component normal to a plane shock front, a reference system can always be found for which all flow velocities are parallel or anti-parallel to the magnetic field and for which the shock is stationary. Such a transformation can be made for each point on the earth's bow shock, and will now be derived. Begin with a reference system in which the bow shock is at rest and in which the angles ψ and α are defined as in the text. We assume non-relativistic transformation so that $\underset{\sim}{B}' = \underset{\sim}{B}$. If initially $\underset{\sim}{v}_W$ is along the z axis and if $\underset{\sim}{B}_0$ is in the X-z plane, the equations to be satisfied are

$$\frac{v'_{W_X}}{v'_{W_z}} = \frac{B_{X_0}}{B_{z_0}} = \tan\psi \quad (\text{i.e. } \underset{\sim}{v}' \parallel \underset{\sim}{B}) \qquad \text{(IV-1)}$$

and

$$v'_{W_z} = v_W - v'_{W_X} \sin\alpha \quad (\text{i.e. shock stationary}); \qquad \text{(IV-2)}$$

these can be readily solved to yield

$$c\beta_0 = \sqrt{{v'_{W_X}}^2 + {v'_{W_z}}^2} = \frac{v_{W_1}}{\cos\psi} \, \frac{1}{1 + \sin\alpha\tan\psi}\,, \qquad \text{(IV-3)}$$

the desired result.

Effects of Diffusion on the Composition of the Solar Corona and Solar Wind

I. Introduction

In this part of the thesis possible effects of radial diffusion on the composition of the solar corona and solar wind are discussed. The initial motivation for this work was the Mariner-2 interplanetary plasma data, which indicate that the ratio by number of alpha particles to protons in the solar wind is often less than 5% and fluctuates widely (Neugebauer and Snyder, 1965). This is also true of the relative abundance of He and H since conditions are such that both He and H are fully ionized. Although the relative abundance of He and H in the lower solar atmosphere is not precisely known, a photospheric value of about 0.1 is indicated by recent solar model computations (Sears, 1964). The value of 0.1 is also consistent with spectroscopic observations of the lower solar atmosphere (Zirin, 1964).

How are we to understand the fluctuations in the solar wind He/H ratio and the apparent difference between the solar wind and photospheric values? In the following a quantitative analysis indicates that substantial changes in the composition of the solar corona and solar wind, as a function of both heliocentric radius and time, are a possible result of radial diffusion under conditions consistent with present knowledge of the corona. We make no attempt here to treat the effects of diffusion on the dynamics of the solar wind; some aspects of this latter problem have been discussed by E. N. Parker (1963), who demonstrated that relative diffusion of alpha particles and protons provide a significant source of heat in the upper corona.

The corona flows outward to form the solar wind. In general this flow is complicated by effects of turbulent mixing and magnetic fields. To obtain a rough quantitative idea of the effects of diffusion, we first analyse in detail a simplified model of the flow. The effects of turbulent mixing and magnetic fields are then discussed.

Assume that the outward flow is essentially radial and that it satisfies the time independent continuity equation $n_t v_t r^2$ = constant, where n_t and v_t are the average number density and velocity of element t at heliocentric radius r. This may be a reasonable approximation to the average behavior of the whole corona over relatively long periods, or to the flow along an individual streamline which may be steady for an extended period. The characteristic time for setting up such a steady flow pattern is of the order of a day, or the time required for the wind to traverse a major portion of the corona. Division of the continuity equation for element A by that for protons yields

$$\left(\frac{n_A}{n_p}\right)_{r_1} = \left(\frac{n_A}{n_p}\right)_{r_0} \left[\frac{(v_A/v_p)_{r_0}}{(v_A/v_p)_{r_1}}\right] . \qquad (1)$$

Clearly, if the term in brackets varies, the relative abundance of element A and protons will change. Since the collision mean free paths of ions in the corona are small relative to the characteristic dimensions, the average relative velocities of particles are governed by the ordinary gas dynamic diffusion equations.

II. Relative Diffusion of Alpha Particles and Protons

Consider first the diffusion of alpha particles. This amounts to a study of He since we will consider only the corona, where He is fully ionized. This will serve to illustrate the general properties of the model. In part III the treatment is extended to heavier elements which may have more than one charge state present.

The Diffusion Equation

The relative diffusion of alpha particles and protons in the corona can be treated to a very good approximation by regarding the corona as a binary mixture of protons and alpha particles, with electrons serving only to neutralize the mixture and to produce a charge separation field. If the magnetic field is assumed radial, its effects on radial diffusion may be neglected, and the relative diffusion velocity in the radial direction may be obtained from the following (Chapman and Cowling, 1952, p. 244)

$$v_p - v_\alpha = v_D = -\frac{n^2}{n_\alpha n_p}[D_{12}]_1\left\{-\frac{d}{dr}\left(\frac{n_\alpha}{n}\right)+\frac{n_\alpha n_p}{n\rho}(m_\alpha - m_p)\frac{d}{dr}\ln P_* + k_T\frac{d}{dr}(\ln T) - \frac{\rho_\alpha \rho_p}{P_* \rho}(F_p - F_\alpha)\right\} \quad (2)$$

where $$[D_{12}]_1 = \frac{3}{16n} \frac{(2kT)^{5/2}}{(e^4 z_\alpha^2)\sqrt{\pi \frac{m_\alpha m_p}{m_\alpha + m_p}}} \frac{1}{\ln[1 + (\frac{4dkT}{e^2 z_\alpha})^2]} \tag{3}$$

$$\simeq \frac{1.1 \times 10^7 \, T^{5/2}}{n} \, . \tag{3^1}$$

In equation (3^1) the slowly varying logarithm has been approximated by 45, its value at about 1.2 solar radii. All of the symbols are self evident, except perhaps

$n = n_p (1 + \frac{n_\alpha}{n_p}) =$ total number density of alpha particles and protons,

$\rho = n_p m_p (1 + 4\frac{n_\alpha}{n_p}) =$ mass density,

$d =$ Debye radius,

$P_* = P_\alpha + P_p =$ total pressure of alpha particles and protons,

$F =$ force/mass = acceleration due to body forces, per particle,

$k_T =$ thermal diffusion coefficient.*

---

* See Chapman and Cowling, 1952, p. 167. In the present case, neglecting terms of order $(\frac{n_\alpha}{n_p})^2$ compared to unity, we have $\frac{n^2}{n_\alpha n_p} k_T \simeq 10 \, [1 - 5\frac{n_\alpha}{n_p}]$.

The subscripts α and p refer to alpha particles and protons, respectively.

We neglect the direct effects of the electrons since it is demonstrated in the appendix to be of the order $(m_e/m_p)^{1/2}$ as compared to the effects of the protons.

However, as another consequence of their small mass, the electrons tend to diffuse rapidly outward (or upward) and set up a charge separation electric field E which must be included in the force term $(F_p - F_\alpha)$. Let us first evaluate E. Consider the general case of N species of ions. Charge neutrality yields

$$n_e = \sum_j n_j z_j , \tag{4}$$

where n_j denotes the number density of species j and the subscript e refers to electrons. Each species must be nearly in static equilibrium under the influence of gravity, of E and of the gradient of its pressure.

$$P_j = n_j k T . \tag{5}$$

Therefore

$$\frac{dP_j}{dr} = n_j(-m_j g + z_j e E) \tag{6}$$

$$\frac{dP_e}{dr} = n_e(-m_e g - e E) . \tag{7}$$

Multiply equation (6) by z_j, equation (7) by (-1) and sum over j and e. Using equation (5) and neglecting $(\frac{m_e}{m_j})$ compared to unity, one obtains

$$e\,E = g\left(\sum_j n_j z_j m_j\right) / \sum_j n_j z_j (z_j + 1) \quad . \tag{8}$$

Note that if there is only one species of ion present, the effective acceleration is

$$F_j = -g/(z_j + 1) \quad , \tag{9}$$

a familiar result (e.g. Spitzer, 1956).

Also, by use of equation (5)

$$P = P_e + \sum_j P_j$$

$$= k\,T \sum_j (z_j + 1) n_j \quad . \tag{10}$$

Furthermore, again neglecting $\frac{m_e}{m_j}$ compared with 1, we obtain

$$\frac{d}{dr}(\ell n\ P) = -g \sum_j m_j n_j / P \ . \tag{11}$$

Now, restricting ourselves to alpha particles, protons and electrons, using $m_\alpha = 4m_p$ and retaining only terms to first order in $\frac{n_\alpha}{n_p}$, we easily obtain

$$e\,E \simeq \frac{gm_p}{2}\,[1 + 5\,\frac{n_\alpha}{n_p} + \ldots] \tag{12}$$

$$\frac{d}{dr}\,(\ell nP) \simeq -\,\frac{gm_p}{2kT}\,[1 + \frac{5}{2}\,\frac{n_\alpha}{n_p} + \ldots] \tag{13}$$

$$\frac{d}{dr}\,(\ell nP_*) \simeq \frac{d}{dr}(\ell nP) - \frac{1}{2}\,(1 - \frac{5}{2}\,\frac{n_\alpha}{n_p})\frac{\partial}{\partial r}(\frac{n_\alpha}{n_p})\;. \tag{14}$$

It is now a matter of algebra to rewrite equation (2) as

$$v_D \simeq -\,\frac{n^2}{n_\alpha n_p}\,[D_{12}]_1\,\Big\{-\,(1 - \frac{1}{2}\,\frac{n_\alpha}{n_p})\frac{d}{dr}(\frac{n_\alpha}{n_p}) - \frac{n_\alpha}{n_p}\,[1 - \frac{3}{2}\,\frac{n_\alpha}{n_p})\,\frac{5m_p g}{2kT} + k_T\,\frac{d}{dr}\,\ell n\,T\Big\} \tag{2^1}$$

where terms of order $(\frac{n_\alpha}{n_p})^2$ have been neglected compared to unity. Equation (2^1) is a good approximation to the more exact ternary equation for this case (Burnett, 1963), the only significant difference if $\frac{n_\alpha}{n_p}$ is small being a difference of perhaps 20% in the thermal diffusion term. Since the thermal diffusion itself is found to be unimportant, this is acceptable.

Consider now the various terms in equation (2^1). We first examine the generalized pressure term which is proportional to g. This can be written

$$(v_D)_{pressure} \simeq \frac{9 \times 10^3 T^{3/2}}{n_p} \frac{r_s^2}{r^2} \left(1 - \frac{1}{2}\frac{n_\alpha}{n_p}\right) \qquad (15)$$

where we have set $g = 2.75 \times 10^4 \left(\frac{r_s}{r}\right)^2$ cm sec^{-2}. If equation (15) is divided by v_p, one obtains

$$\left(\frac{v_D}{v_p}\right)_{pressure} \simeq \frac{9 \times 10^3 T^{3/2}}{n_p v_p r^2} r_s^2 \left(1 - \frac{1}{2}\frac{n_\alpha}{n_p}\right). \qquad (16)$$

This is a very useful form since we have assumed that $n_p v_p r^2 \simeq$ constant and has a value that can readily be obtained from the Mariner-2 data. For a nominal solar wind proton flux of 3×10^8 cm^{-2}sec^{-1} at 1 AU (Snyder and Neugebauer, 1962), we have

$$\left(\frac{v_D}{v_p}\right)_{pressure} \simeq 6 \times 10^{-10} T^{3/2}\left(1 - \frac{1}{2}\frac{n_\alpha}{n_p}\right). \qquad (17)$$

It is evident from equation (17) that the pressure term gives rise to $v_D/v_p \simeq 1$ for nominal coronal temperatures of $1 - 2 \times 10^6$ °K.

The Thermal Diffusion Term

From equation (2) and the definition of k_T, the ratio R_{TP} of the thermal and pressure terms can be written

$$R_{TP} = -1.2 \times 10^4 \left(\frac{r}{r_s}\right)^2 \frac{dT}{dr} \left(1 - 4\frac{n_\alpha}{n_p}\right) \tag{18}$$

where again terms of order $\left(\frac{n_\alpha}{n_p}\right)^2$ have been neglected.

We note first that, although the temperature gradient in the solar corona is not well known, it is probably of the order of -10^{-5} ^oK cm^{-1} at $\frac{r}{r_s} \simeq 1.1$ (Billings and Lilliequist, 1963). Thus in this region of the corona R_{TP} is positive and has a value of perhaps 10-20%, so that thermal diffusion is probably relatively unimportant in the lower corona.

In the chromosphere, on the other hand, $\frac{dT}{dr}$ is positive and may be of the order of 10^{-4}-10^{-3} ^oK cm^{-1}. R_{TP} is therefore negative and may be of the order of unity or larger. However, the larger densities and lower temperatures in the chromosphere and lower solar atmosphere suggest that the solar wind and diffusion are not important in determining its characteristics. Our attention, therefore, will continue to be confined mainly to the corona.

The Concentration Term

This term is in general difficult to deal with since it depends on the concentration gradient which in turn is determined by the diffusion. Under the assumption that the continuity equation (1) is valid, however, $\frac{d}{dr}\left(\frac{n_\alpha}{n_p}\right)$ may be related to $\frac{d}{dr}\left(\frac{v_D}{v_p}\right)$ and a solution for (v_D/v_p) may be found. Thus,

$$\frac{d}{dr}\left(\ell n\,\frac{n_\alpha}{n_p}\right) = \frac{1}{1 - v_D/v_p}\,\frac{d}{dr}\left(\frac{v_D}{v_p}\right) \tag{19}$$

and R_{CP}, the ratio of the concentration and pressure terms in equation (2^1) may be written

$$R_{CP} = 1.2 \times 10^3 T \left(\frac{r}{r_s}\right)^2 \frac{1}{1 - v_D/v_p}\,\frac{d}{dr}\left(\frac{v_D}{v_p}\right) \tag{20}$$

which is correct to terms of order $\frac{n_\alpha}{n_p}$. First note that R_{CP} is small at low temperatures, so that v_D/v_p is essentially $(v_D/v_p)_{pressure}$. This can be verified by substituting $\left(\frac{v_D}{v_p}\right)_{pressure}$ from equation (17) into R_{CP} and noting that for $\frac{dT}{dr}$ of the order of $-10^{-5}\ {}^oK\ cm^{-1}$, $R_{CP} \lesssim \frac{0.1}{1 - v_D/v_p}$. This is small as long as $(v_D/v_p)_{pressure} \ll 1$, or for $T \lesssim 1.3 \times 10^6\ {}^oK$. However, as (v_D/v_p) approaches unity, R_{CP} becomes large and the concentration term must be included.

We now proceed to a more general treatment. The complete expression for diffusion, to order $\frac{n_\alpha}{n_p}$, may be written in the form

$$\left(\frac{v_D}{v_p}\right) = \left(\frac{v_D}{v_p}\right)_{\text{pressure}} [1 + R_{TP} + R_{CP}]$$

$$= \frac{9.2 \times 10^3 T^{3/2} r_s^{\ 2}}{n_p v_p r^2} \left[1 - \frac{n_\alpha}{n_p}\right] \times \tag{22}$$

$$\times \left\{1 - 1.2 \times 10^4 \left(\frac{r}{r_s}\right)^2 \frac{dT}{dr}\left(1 - \frac{4n_\alpha}{n_p}\right) + 1.2 \times 10^3 \left(\frac{r}{r_s}\right)^2 \frac{T}{(1 - v_D/v_p)} \frac{d}{dr}\left(\frac{v_D}{v_p}\right)\right\}.$$

Given $T(r)$ and the value of $\frac{n_\alpha}{n_p}$ at some radius, equation (22) could in principle be solved for (v_D/v_p) as a function of r. Alternatively, fixing r, $\frac{n_\alpha}{n_p}$, $\frac{dT}{dr}$ and writing $\frac{d}{dr}\left(\frac{v_D}{v_p}\right)$ as $\frac{dT}{dr} \cdot \frac{d}{dT}\left(\frac{v_D}{v_p}\right)$, equation (22) may be solved for v_D/v_p as a function of T. We follow the latter approach and write equation (22) as

$$\left(\frac{v_D}{v_p}\right) = AT^{3/2}\left[B - \frac{CT}{\left(1 - \frac{v_D}{v_p}\right)} \frac{d}{dT}\left(\frac{v_D}{v_p}\right)\right] \tag{23}$$

where A, B and C are now constants determined from equation (22) and dependent on the assumed values of r, $\frac{n_\alpha}{n_p}$ and $\frac{dT}{dr}$. Equation (23) is readily solved for (v_D/v_p). We are interested in the case for the solar corona, where $\frac{dT}{dr} \simeq -10^{-5}\ {}^{o}K\ cm^{-1}$ and $R_{TP} < 1$. Thus B and C are both positive. Defining the new function $y(T) = [\frac{v_D}{v_p} - 1]^{-1}$, one finds that equation (23) is a linear equation for y and it is readily solved by elementary techniques. Physically, it is reasonable to fix the constant of integration by requiring (v_D/v_p) to go to zero as T approaches zero. In terms of the parameters $\beta = \frac{2}{3}\frac{B}{C}$ and $X = \frac{2}{3AC} T^{-3/2}$, one eventually obtains

$$(\frac{v_D}{v_p}) = 1 - \frac{X^{\beta} e^{-X}}{\Gamma(\beta + 1) - \gamma(\beta + 1,\ X)} . \qquad (24)$$

Use has been made of the incomplete and complete gamma functions, defined by the relations $\gamma(a,\ X) = \int_0^X t^{a-1} e^{-t} dt$ and $\Gamma(a) = \gamma(a,\ \infty)$. In the limit of small T, equation (24) becomes

$$(\frac{v_D}{v_p}) \simeq A B T^{3/2} \qquad (25)$$

and, as one expects, the concentration term is negligible. The behavior of v_D/v_p as a function of T is sketched in Figure 1 for $\frac{n_\alpha}{n_p} = 0.1$, $r/r_s \simeq 1.1$ and for two nominal values of $\frac{dT}{dr}$. It is immediately apparent that the diffusion velocity v_D can be an appreciable fraction of the proton velocity in the corona, where

Figure 1

The relative diffusion velocity of alpha particles and protons at $\frac{r}{r_s} = 1.1$ as a function of temperature for a solar wind proton flux of $n_p v_p = 3 \times 10^8$ $cm^{-2} sec^{-1}$ at 1 AU and for $n_\alpha / n_p = 0.1$.

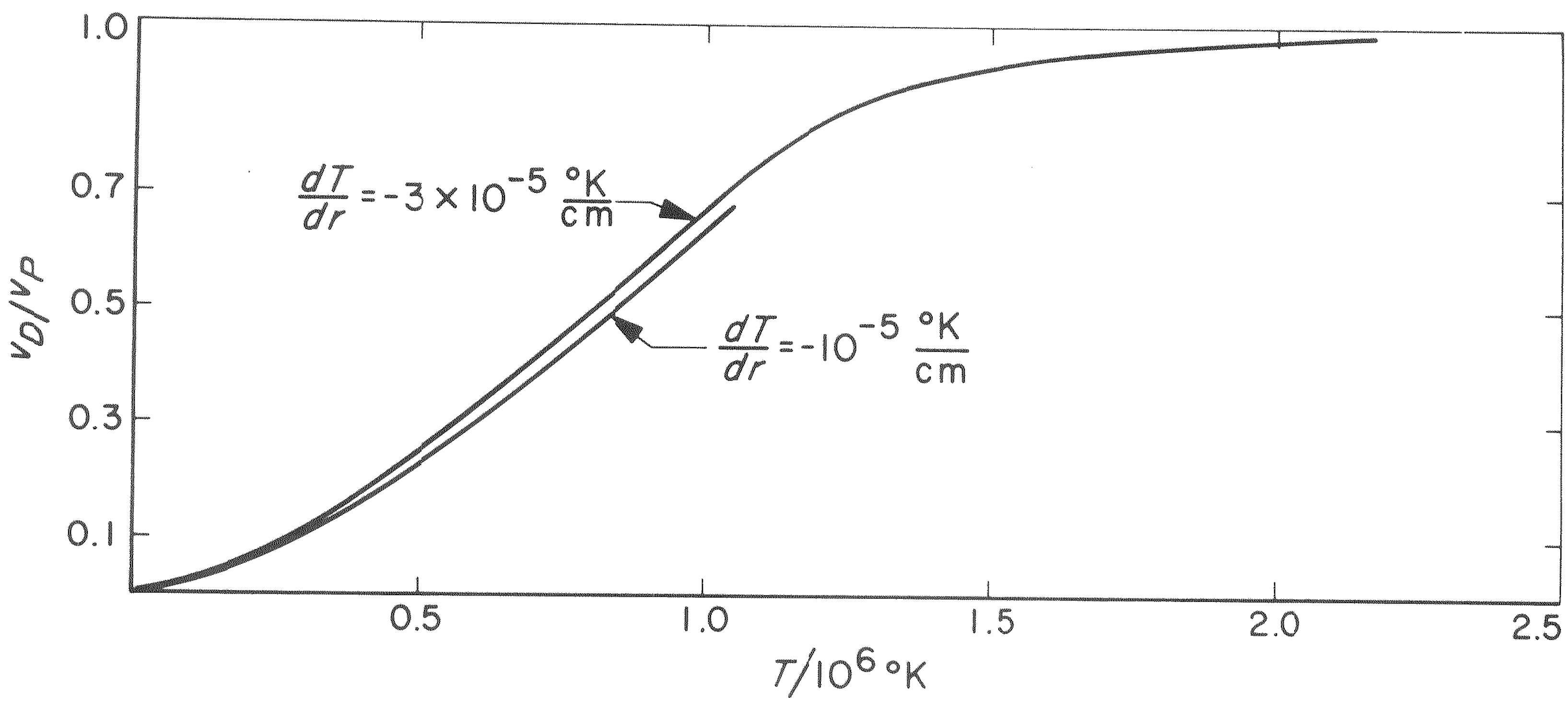
1.0
0.7
0.5
0.3
0.1
v_D/v_P
$\frac{dT}{dr} = -3 \times 10^{-5} \frac{°K}{cm}$
$\frac{dT}{dr} = -10^{-5} \frac{°K}{cm}$
0.5
1.0
1.5
2.0
2.5
$T/10^6 °K$

Figure 1

$T \simeq 1\text{-}2 \times 10^{0}\ {}^{o}K$. Figure 1 also illustrates the small dependence on the coronal temperature gradient.

We go on to consider the diffusion of other ions relative to protons and consider the effects of diffusion on the composition in section IV.

III. Consequences for Ions Other Than Alpha Particles

In part II we discussed the relative diffusion of alpha particles and protons. A similar analysis can be carried out for any element that is present in only one charge state. For most of the heavier elements, however, this is not true and the possibility of transitions between the various charge states present must be taken into account. In this section numerical results are given for Ni and Fe, although the results are readily applied to other elements.

We must utilize a different approximation from that used for alpha particles since we can treat at most a ternary gas of which one of the components has negligible mass (i.e. electrons). The approximation used here is that the coronal gas is a ternary mixture of the heavy ions under consideration, protons and electrons. Furthermore, the concentration of the heavy element is neglected. We are then effectively neglecting collisions with the alpha particles and heavy ions. The heavy ions are certainly less than 10^{-3} of the gas by number so their neglect is clearly justified. In the appendix it is shown that the effect of alpha particles is of the order of $8 \frac{n_\alpha}{n_p}$ compared to the effect of protons. If $\frac{n_\alpha}{n_p} \simeq .1$, this indicates that, while protons are probably more important, the effect of alpha particles is by no means negligible. Since the alpha particles are drifting backward relative to the protons at a velocity v_D, it is expected that neglecting the alpha particles somewhat underestimates or overestimates v_{D_i}, the ion diffusion velocity, as v_D is greater than or less than v_{D_i}.

The diffusion equation for this situation may be derived exactly as that for the alpha particles. The electric field and pressure gradient are given by equations (12) and (13) for ion i can then be written

$$v_{D_i} = - [D_{12}]_{1_i} \left[\frac{d}{dr} \ln\left(\frac{n_i}{n_p}\right) + \left\{1 + z_i - 2\frac{m_i}{m_p}\right\}\left(-\frac{gm_p}{2kT}\right) \right.$$

$$\left. \alpha_i \frac{d}{dr} \ln T \right] , \qquad (26)$$

where the notation is the same as in equation (2) except for:

the subscript i refers to the ion under consideration.

$$[D_{12}]_{1_i} = [D_{12}]_1 \cdot \left[\frac{3.6}{z_i^2} \left(1 + \frac{m_p}{m_i}\right)^{1/2} \right] ,$$

$$\simeq \frac{4 \times 10^7 \, T^{5/2}}{n} \cdot \frac{1}{z_i^2} \left(1 + \frac{m_p}{m_i}\right)^{1/2} ,$$

$$n = n_p + n_i = n_p ,$$

$$\alpha_i \simeq 5.3 z_i^2 \quad \left(\text{in the limit } \frac{m_p}{m_i} << 1\right) .$$

z_i = ionic charge in units of e.

Proceeding precisely as in the alpha particle case, we obtain

$$\left(\frac{v_{D_i}}{v_p}\right)_{pressure} \simeq \frac{6.5 \times 10^3 T^{3/2} r_s^2}{n_p v_p r^2} \frac{\left\{2 \frac{m_i}{m_p} - z_i - 1\right\}}{z_i^2 \sqrt{\frac{m_i}{m_p}} \left(\frac{1}{m_i/m_p + 1}\right)} \tag{27}$$

or, again for a nominal solar wind proton flux $n_p v_p \simeq 3 \times 10^8 \text{ cm}^{-2} \text{sec}^{-1}$ at 1 AU,

$$\left(\frac{v_{D_i}}{v_p}\right)_{pressure} \simeq .5 \times 10^{-9} T^{3/2} \frac{\left\{2 \frac{m_i}{m_p} - z_i - 1\right\}}{z_i^2 \sqrt{\frac{m_i}{m_p}} \left(\frac{1}{m_i/m_p + 1}\right)} . \tag{28}$$

It is clear that for a typical ion such as FeXIII, this term is of the order of unity for typical coronal temperatures of $1 - 2 \times 10^6$ °K.

Similarly, one obtains for $(R_{TP})_i$, the ratio of the thermal and pressure terms,

$$(R_{TP})_i \simeq -3.2 \times 10^4 \frac{z_i^2}{\left[2 \frac{m_i}{m_p} - z_i - 1\right]} \left(\frac{r^2}{r_s^2}\right) \frac{dT}{dr} . \tag{29}$$

Again, as for alpha particles, setting $\frac{dT}{dr} \sim -10^{-5}$ °K cm^{-1} leads to $(R_{TP})_i < 1$, and the pressure term dominates.

Because of transition between the various ionization stages of a given element, $n_i v_i r^2$ is no longer a constant and the concentration term must be handled in a slightly different manner than for alpha particles. We may write, for a given element t,

$$n_t v_t r^2 = \text{constant} \tag{30}$$

where

$$v_t = \sum_{\text{element}} n_i \tag{31}$$

$$v_t = \sum_{\text{element}} \frac{n_i}{n_t} v_i \, . \tag{32}$$

In general $n_i/n_t = f_i$ will be a complicated function of r, depending on both $v_t(r)$ and $T(r)$. For most ions, however, it may be considered that the time scale for approaching ionization equilibrium in the corona is short enough that f_i corresponds to the equilibrium value for $T(r)$.

Proceeding as before and utilizing equation (30), $(R_{CP})_i$ can be written

$$(R_{CP})_i = \frac{6 \times 10^3\, T}{\left\{2\frac{m_i}{m_p} - z_i - 1\right\}} \left(\frac{r}{r_s}\right)^2 \left\{\frac{d}{dr} \ln f_i + \frac{1}{1 - \frac{v_{D_t}}{v_p}} \frac{d}{dr} \left(\frac{v_{D_t}}{v_p}\right)\right\} \tag{33}$$

where $v_{D_t} = \sum f_i v_{D_i}$. We may again write

$$\frac{v_{D_i}}{v_p} = \left(\frac{v_{D_i}}{v_p}\right)_{\text{pressure}} \left[1 + (R_{TP})_i + (R_{CP})_i\right], \tag{34}$$

but since $(R_{CP})_i$ depends on v_t, this cannot be solved for $\frac{v_{D_i}}{v_p}$.

Multiply equation (34) by f_i and sum over i for a given element t. The resulting equation may be written

$$\left(\frac{v_{D_t}}{v_p}\right) = A_t T^{3/2} \left[B_t + C_t \frac{T}{(1 - v_{D_t}/v_p)} \frac{d}{dT}\left(\frac{v_D}{v_p}\right) + G_t T\right] \tag{35}$$

in analogy with equation (23), where

$$A_t = \frac{6.5 \times 10^3 r_s^{\,2}}{n_p v_p r^2} \sum_i f_i(T) \frac{\left\{2\frac{m_i}{m_p} - z_i - 1\right\}}{z_i^{\,2}\sqrt{\frac{m_i}{m_p}\left(\frac{1}{m_i/m_p + 1}\right)}} \tag{36}$$

$$B_t = 1 - 3.2 \times 10^4 \left(\frac{r}{r_s}\right)^2 \frac{dT}{dr} \sum_i \frac{f_i(T)\, z_i^{\,2}}{\left[2\frac{m_i}{m_p} - z_i - 1\right]} \tag{37}$$

$$C_t = 6 \times 10^3 \left(\frac{r}{r_s}\right)^2 \frac{dT}{dr} \sum_i f_i(T) \frac{1}{\left[2\frac{m_i}{m_p} - z_i - 1\right]} \tag{38}$$

$$G_t = 6 \times 10^3 \left(\frac{r}{r_s}\right)^2 \frac{dT}{dr} \sum_i \frac{df_i/dT}{\left[2\frac{m_i}{m_p} - z_i - 1\right]} \quad . \tag{39}$$

Since the f_i are in general complicated functions of temperature, A_t, B_t and C_t are not constants and no simple solution is possible. However, we saw that for alpha particles the concentration term was negligible for $v_p/v_p \ll 1$, and in that region $\left(\frac{v_D}{v_p}\right) \simeq ABT^{3/2}$. This is independent of whether or not A and B are constants and the approximation should be valid in the present case also.

Using equilibrium values of f_i determined from tables in Shklovskii (1963), $\left(\frac{v_{D_t}}{v_p}\right) \simeq A_t B_t T^{3/2}$ can readily be computed for Fe and Ni. If $dT/dr \simeq -10^{-5}$ $^oK\ cm^{-1}$, it is found that in both cases (v_{D_t}/v_p) is about 0.5 for T in the range 1 to 1.5×10^6 ^oK. Although the calculation is much cruder than was the case for alpha particles, we may conclude that diffusion is important for Fe, Ni and probably other elements present in the corona.

IV. The Composition as a Function of Radius

We are now in a position to discuss the composition as a function of radius for the simple time independent solar wind model. Following paragraphs discuss briefly the effects of magnetic fields and turbulent mixing on the conclusions of the model. We will discuss the behavior of the alpha particle to proton ratio, but it is clear from section III that the conclusions should apply also to other ions.

It is plausible that the relative diffusion velocity go to zero at large radii, either because the diffusion equations remain valid and the temperature falls, or because tangled magnetic fields in the solar wind prevent diffusion. It is then indicated that a large difference in the relative abundance of He and H occur between the corona and the solar wind. From equation (1) and Figure 1 we see that for a coronal temperature of 1.5×10^6 °K the difference may be as large as a factor of ten in relative abundance.

Consider now the reasonable coronal temperature profile shown in Figure 2a. From equation (24), we may expect v_D/v_p to be as shown in Figure 2b and the behavior of n_α/n_p as indicated by the solid line in Figure 2c. The photospheric value of n_α/n_p has been taken to be 0.1, although the behavior is expected to be typical. As we proceed outward, the large temperature gradient in the chromosphere forces v_D/v_p to be negative and decreases n_α/n_p slightly. In the corona, the temperature is high and n_α/n_p is increased. Finally, at larger radii v_D/v_p returns to zero and n_α/n_p returns to its photospheric value. It is clear that in this model the solar wind and photospheric abundances should be

Figure 2

(a) Radial temperature profile assumed.

(b) Expected relative diffusion velocity as a function of height above photosphere, and

(c) Calculated relative alpha particle abundance as a function of height above photosphere.

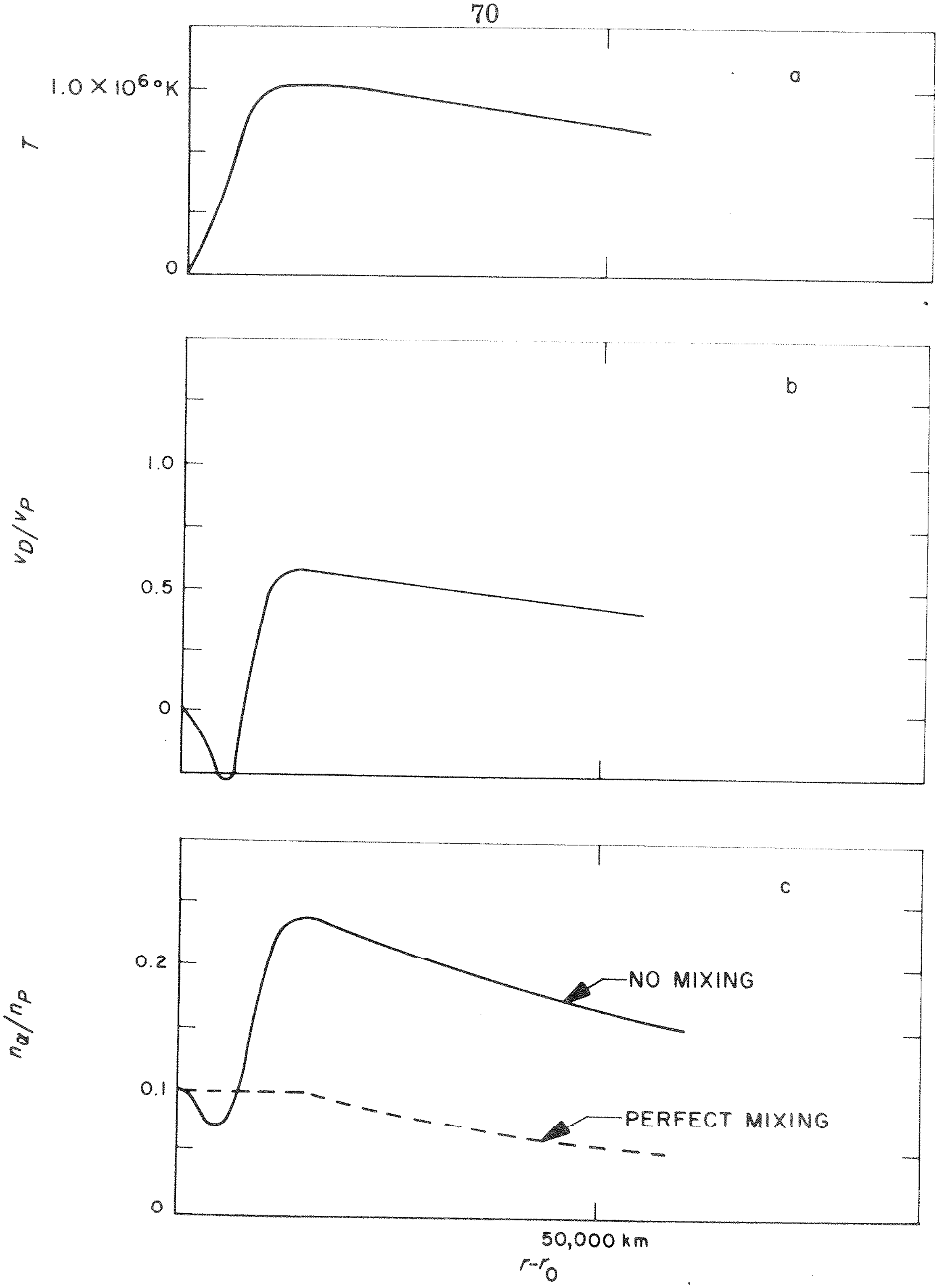
1.0 X 10⁶ °K
T
0
a
b
1.0
v_D/v_P
0.5
0
c
0.2
n_α/n_P
0.1
0
NO MIXING
PERFECT MIXING
50,000 km
$r-r_0$

Figure 2

essentially constant and identical. Nonetheless, it has been demonstrated that diffusion can change the composition with height above the photosphere. We go on to consider possible effects of transverse magnetic fields and turbulent mixing.

The Effect of a Magnetic Field

A magnetic field impedes diffusion of charged particles normal to it, so that diffusion tends to be mainly along the field lines. The ratio of the diffusion constants for diffusion normal to and parallel to a magnetic field is about $\left(\frac{1}{1 + \lambda^2/r_g^2}\right)$, where r_g is the particle gyroradius and λ is the collisional mean free path. For the corona, $\lambda \simeq 10^7 - 10^8$ cm and $r_g \simeq 10^3$ cm (Lüst, 1962), yielding 10^{-8} for the relative importance of perpendicular and parallel diffusion. Clearly, we can neglect perpendicular diffusion, and the above calculations are valid only if the magnetic field in the corona is essentially radial. There is theoretical reason to believe that the solar wind tends to drag out the coronal field so that it forms a spiral pattern that is radial near the sun (Parker, 1963). This is supported by radio observations of the outer corona (Hewish, 1963). It is perhaps most reasonable that the field lines are usually parallel (or anti-parallel) to the flow velocity, but that occasional transverse loops are transported out by the solar wind. Then the average diffusion may then be approximated as discussed above, but that occasional "traps" occur in the wind which impede diffusion and which may have locally higher alpha particle abundance. It is reasonable, then, that occasionally the relative alpha particle abundance in the solar wind may be substantially larger than the photospheric abundance, although it may average somewhat less.

A somewhat different effect of the magnetic field is the possibility that it may not allow the solar wind to flow out evenly and may "channel" the wind (Davis, 1963). The above arguments would still be essentially valid, except that the equation of continuity may have to be modified to $nvr^2 a(r)$ = constant where $a(r)$ is a measure of this effect of the magnetic field. This would leave equation (1) unchanged, but would change the total diffusion velocity at a radius r by the factor $a(r)/a(r = 1\ \mathrm{AU})$, since $n_p v_p r^2$ is no longer constant. This effect is unlikely to change the qualitative nature of the results.

It should further be noted that a magnetic field should tend to stabilize the flow pattern against convection.

The Effects of Mixing

Turbulent mixing within the solar atmosphere will act to smooth out the changes in composition indicated in Figure 2c. Some of the mixing may be effected by flares, spicules and other solar activity. Furthermore, even in the absence of these mechanisms, the predicted increase in alpha particle abundance in the corona would tend to make it unstable against convection. That is, the regions of large alpha particle abundance may tend to sink because of their higher density. The mixing may be regarded as effectively spreading out the effects of diffusion over a larger part of the solar atmosphere, tending to reduce any changes in composition. If the mixing acted only below the region of rapid diffusion and kept

$\frac{n_\alpha}{n_p} \simeq 0.1$ in this region, the average run of $\frac{n_\alpha}{n_p}$ with radius may be somewhat as indicated by the dashed line in Figure 2c. It is also to be expected that the mixing does not act smoothly and continuously, so that we expect substantial fluctuations in the composition with time as a result of diffusion and mixing occurring together.

V. Conclusions

It seems reasonable to conclude that diffusion has a substantial effect on the composition of the solar wind. If the proposed model is taken to represent the time averaged properties of the outward coronal flow pattern, we may conclude that the average abundances of alpha particles and heavier ions relative to protons in the solar wind may be less than their photospheric values. Also, these abundances may be substantially enhanced in the lower corona, near the coronal temperature maximum. In other words, the solar wind leaves the ions behind in the lower corona, tending to increase their coronal abundance and to decrease their solar wind abundance.

Transverse magnetic fields and turbulent mixing, when considered in conjunction with the expected rapid diffusion, probably cause substantial fluctuations in the composition as a function of heliocentric radius and time.

The observed values of the He/H ratio, obtained from the Mariner-2 data, which indicate values of $n_\alpha/n_p \simeq 0.05$ with wide fluctuations can therefore be reconciled with a photospheric He/H ratio of 0.1. It is tempting to speculate that spectroscopic evidence of enhanced Fe abundances in the lower corona (Pottasch, 1963 a, b) may be further confirmation of this model.

Appendix

Consider the relative importance of two species on the diffusion of a third through them. Since diffusion is a collisional phenomena, the relative importance of two species should be of the order of the inverse ratio of the near deflection times t_D, as defined in Spitzer (1956), for a test particle of the third species. Thus, from the definition of t_D

$$q_{12} = \left(\frac{t_{D_1}}{t_{D_2}}\right)^{-1} = \frac{n_1 z_1^2 \left[\Phi\left(\frac{m_1 v^2}{kT}\right) - G\left(\sqrt{\frac{m_1 v^2}{kT}}\right)\right]}{n_2 z_2^2 \left[\Phi\ \frac{m_2 v^2}{kT} - G\left(\sqrt{\frac{m_2 v^2}{kT}}\right)\right]} \tag{A-1}$$

where $\Phi(X) = \frac{2}{\sqrt{\pi}} \int_0^X e^{-y^2} dy$ and $G(X) = \frac{\Phi(X) - X\Phi'(X)}{2X^2}$.

Since we are interested in slowly diffusing particles whose masses are in general larger than those of the field particles, $\sqrt{\frac{mv^2}{kT}} < 1$ and to a good approximation $\Phi(X) - G(X) \simeq \frac{4}{3\sqrt{\pi}} X$. Therefore,

$$q_{12} \simeq \frac{n_1 z_1^2 \sqrt{m_1}}{n_2 z_2^2 \sqrt{m_2}} . \tag{A-2}$$

It is clear that the relative importance of electrons and protons in $q_{ep} \simeq \sqrt{\frac{m_e}{m_p}} \simeq \frac{1}{40}$, and the relative importance of protons and alpha particles on the diffusion of heavier ions is $q_{\alpha p} \simeq 8\left(\frac{n_\alpha}{n_p}\right)$.

References for A Model of Fermi Acceleration at Shock Fronts

Anderson, K. A., H. Harris and R. J. Paoli, University of California at Berkeley Space Sciences Laboratory Report, Series 5, No. 50 (1964).

Axford, W. I. and G. C. Ried, J. Geophys. Res. 68, 1793 (1963).

Bazer, J. and W. B. Ericson, Astrophys. J. 129, 758 (1959).

Bridge, H., A. Egidi, A. Lazarus, E. Lyon and L. Jacobson, Cospar Meeting, Florence, Italy (unpublished) (1964).

Fan, C. Y., G. Gloeckler and J. A. Simpson, Phys. Rev. Letters 13, 149 (1964).

Frank, L. and J. Van Allen, J. Geophys. Res. 69, 4923 (1964).

Fredricks, R. W., F. L. Scarf and W. Bernstein, J. Geophys. Res. 70, 21 (1965).

Freeman, J. W., J. Van Allen and L. J. Cahill, J. Geophys. Res. 68, 2121 (1963).

Ginzburg, V. and S. Syrovatsky, "The Origin of Cosmic Rays", Macmillan, New York (1964).

Jokipii, J. R. and Leverett Davis Jr., Phys. Rev. Letters 13, 739 (1964).

Montgomery, M. D., S. Singer, J. P. Conner and E. E. Stogsdill, Phys. Rev. Letters 14, 209 (1965).

Ness, N. F., C. S. Scearce and J. B. Seek, J. Geophys. Res., 69, 3531 (1964).

Parker, E. N., Phys. Rev. 109, 1328 (1958).

Snyder, C., M. Neugebauer and V. Rao, J. Geophys. Res. 68, 6361 (1963).

Sonett, C. P., D. S. Colburn, L. Davis Jr., E. J. Smith and P. J. Coleman, Phys. Rev. Letters 13, 153 (1964).

Spitzer, L. Jr., "Physics of Fully Ionized Gases", Interscience Publishers, New York (1957).

Swann, W. F. G., Phys. Rev., 43, 217 (1933).

Van Allen, J. and L. Frank, Nature, 184, 219 (1959).

Wentzel, D. G., Ap. J., 137, 135 (1963).

References for Effects of Diffusion on the Composition of the Solar Corona and Solar Wind

Billings, D. and Lilliequist, C., Ap. J. 137, 16 (1963).

Burnett, D., Private Communication (1963).

Chapman, S. and Cowling, T. G., "The Mathematical Theory of Non-Uniform Gases", 2nd ed., Cambridge University Press, (1952).

Davis, L., "Proceedings of AAS-NASA Symposium on the Physics of Solar Flares", Washington, D.C., (1964).

Hewish, A., Mon. Not. Roy. Astron. Soc. 118, 534 (1958).

Lüst, R., Space Science Reviews, 1, 522 (1962).

Neugebauer, M. and Snyder, C., Private Communication (1965).

Parker, E. N., "The Solar Corona: Proceedings of I. A. U. Symposium No. 16", 1961, Academic Press, New York (1963).

Parker, E. N., "Interplanetary Dynamical Processes", Interscience, New York, (1963).

Schwarzschild, M., "Structure and Evolution of the Stars", Princeton University Press, Princeton, N. J., (1958).

Sears, R. L., Ap. J. 140, 477, (1964).

Shklovskii, E., "Fysika Solnechnoi Koroni", pp. 236-238, Moscow (1962).

Snyder, C. and Neugebauer, M., Technical Memorandum No. 33-111 Jet Propulsion Laboratory of Calif. Inst. of Tech., Pasadena, Calif. (1962).

Spitzer, L., "Physics of Fully Ionized Gases" New York, : Interscience Publishers Inc. (1965).

Pottasch, S., Ap. J. 137, 945 (1963a)
Mon. Not. Roy. Astron. Soc. 125, 544 (1963b).

Zirin, H., Ap. J. 140, 1216 (1964).